Thermal Effects During Welding On SiC/Al Composite

Avinash Kumar Agarwal
B.Tech., I.I.T.(Bombay)
1987

A Thesis submitted to the faculty
of the Oregon Graduate Center
in partial fulfillment of the
requirements for the degree
Master of Science
in
Materials Science and Engineering

June, 1989

to

my family

The thesis "Thermal Effects During Welding On SiC/Al Composite" by Avinash K. Agarwal has been examined and approved by the following examination committee:

Dr. Jack H. Devletian
Professor
Thesis Advisor

Dr. William E. Wood
Professor

Dr. Rao Gudimetla
Assistant Professor

ACKNOWLEDGEMENTS

I wish to express my sincere gratitude for my advisor Dr. Jack Devletian for his support and guidance during this project. He was a wonderful person to work with. I also thank Dr. William Wood and Dr. Gudimetla Rao, for reviewing my thesis, and giving some valuable suggestions.

I gratefully acknowledge the support of Welding Research Council and Oregon Graduate Center for this project. I also thank US army and DWA for providing the SiC/Al composite used in this study.

Ken Burns provided invaluable help with the gleeble, which is sincerely appreciated. Finally, a heart felt sense of gratitude for my friends Vivek, Deva, Sudarshan, Rajesh, CVR and Lu Fang for all their help.

TABLE OF CONTENTS

List of Tables

List of Figures

Abstract

Thermal Effects During Welding On SiC/Al Composite

Avinash K. Agarwal
Oregon Graduate Center

Advisor: Dr.Jack H. Devletian

Silicon carbide reinforced aluminum composites have generated much interest among researchers in recent years, for their applications in the aerospace industry. But, to date, very limited data has been published on the welding of this composite. Thus, a systematic study was undertaken to study various changes in the structure and properties of discontinuous SiC whisker reinforced 6061 aluminum matrix composite due to heat flow during fusion welding. Unreinforced 6061 Al was used as a basis for comparing the changes in the composite.

In the heat affected zone (HAZ), simulated on the Gleeble, the composite exhibited softening similar to that observed in 6061 Al. The lowering in the strength and hardness in the HAZ was measured as a function of the peak temperature. The composite maintained its much superior strength over the unreinforced 6061 aluminum for all temperatures up to the solidus. Analysis of microstructure confirmed that there was no reaction between SiC and aluminum in the simulated HAZ, and thus there was little change at the interface. On the other hand, in the real and simulated fusion zone studies, porosity and the presence of free silicon was observed, implying the reaction between SiC and Al matrix. Transmission electron microscopy was used to analyze the changes in the inter-

face and the highly dislocated matrix. Energy dispersive X-ray analysis demonstrated that silicon had formed at the interface and diffused into the matrix. These results suggest that commercial welding of this composite is possible if heat input and superheating temperatures in the weld pool can be minimized.

I. Introduction

The ever increasing need of the aerospace and the automobile industries for materials with higher strength, in addition to high specific stiffness, led material scientists to look beyond the realm of conventional alloys, which led to the development of metal matrix composites (MMC). Discontinuous silicon carbide reinforced aluminum matrix composite is particularly desirable due to its (1) high strength (2) stiffness to density ratio (3) relatively better machinability and workability compared to other composites, (4) good thermal conductance and corrosion resistance. Also, recent advances in processing techniques, which have made this composite attractive economically, have led to extensive research into its structure and properties.

The factors determining the properties of this composite are: (i) the 6061 Al matrix microstructure, (ii) the amount and geometry of SiC, the strengthening phase and (iii) the interface between SiC and Al. These three factors are interdependent, and the final strengthening is brought about by the combined effect of each of these factors. Good compatibility between the strengthening phase and the matrix is a must in any composite, hence the interface characteristics are of great importance. The effect of any treatment, thermal or mechanical, on each of these factors should be taken into account while evaluating this composite. In the past few years, with the help of high resolution and analytical electron microscopy and Auger electron spectroscopy, considerable insight has been gained about the microstructure and the interface characteristics.

Wide spread applications of SiC/Al composite as a structural material necessitates a reliable and economical welding technology. Very little data has been published so far about the fusion welding of this important composite. A thorough understanding of the various implications of welding SiC/Al composite is long overdue.

Thermal exposures during welding has a strong impact on the mechanical properties. Thus it becomes very important to know the extent of the changes in properties, if this composite is to be used as a welded material for structural applications. Also, obtaining an understanding of the weld induced microstructural changes, is essential for improving the properties of a welded SiC/Al composite, either by a more judicious choice of welding parameters or by post-welding treatment.

The thermal flow experienced during welding was simulated using (1) a Gleeble and (2) a furnace. After giving different thermal cycles, to reproduce different regions of the heat affected zone, the mechanical properties were evaluated. All tests and analysis carried out on the composite were also repeated on 6061 aluminum alloy, which forms the matrix in the composite. This was to obtain a basis for comparing the changes in the composite. Finally microstructural analysis was performed using optical and electron microscopy. Thus, the main objective of this project was to obtain a fundamental understanding of the structural and property changes due to thermal exposures during welding.

II. Literature Review

A. Composites

Composite is a very general term, referring to any combination of two or more materials on a macroscopic scale. Material scientists currently associate it with tailor made materials possessing a set of properties, which cannot be provided by conventional alloys. For example, it is very difficult to find an alloy which provides high strength, along with high stiffness and very low density.

Basically, a composite has a bulk matrix material and a strengthening phase, which has a high stiffness and high strength. It is either in the form of long continuous fibers, or discontinuous particulate or whiskers. The composites reinforced with long continuous fibers are very difficult to fabricate, and are hence expensive. On the other hand, those reinforced by discontinuous whiskers or particulates are relatively easier to fabricate and machine, and hence are more economical and much more popular.

The composites can be classified into three categories:-

i) The polymer matrix composites, which are already being used for various structural applications. They can only be used up to 300°C .

ii) The ceramic matrix composites, which are specifically for high temperature applications.

iii) The metal matrix composites, which are becoming increasingly popular due to plethora of properties they can offer [1].

MMC's not only offer higher strength and stiffness than the traditional

engineering alloys, but also good corrosive resistance and conductivities [2]. Currently, aluminum alloys, magnesium, titanium alloys are being used as matrix materials in various composites. These are reinforced by high stiffness high strength materials like silicon carbide, graphite, boron, boron carbide, alumina etc.

B. SiC/Al Composite

During the last decade, discontinuous silicon carbide reinforced 6061 aluminum matrix composite has emerged as one of the leading MMC. This has been mainly due to advances in the processing technology and the cheap availability of SiC [3]. SiC whiskers are grown from ground rice hulls by pyrolysis of Si and carbon. Two fabrication process are currently being used for making SiC/Al composites. The powder metallurgy method involves mixing Al powder with SiC particulates or discontinuous whiskers. After mixing, it is hot-pressed and worked to the required shape. Liquid metal infiltration involves infiltrating the SiC preform with molten Al [4] .

This composite is as light as Al, and at the same time it offers much higher strength and stiffness [5,6]. It also offers corrosion resistance and thermal conductivity and relatively better workability and machinability than the other composites [Table I] . This unique class of advanced engineering materials can be easily forged, superplastically formed and precision machined into complex shapes, which has already qualified it for use in aerospace structures, inertial guidance systems and light weight optical assemblies [7,8] .

The mechanical properties have been studied at various temperatures and SiC percentages. The SiC/Al MMC's have much better higher temperature stability than 6061 Al. Also SiC particulate composites are less creep resistant than

whisker reinforced [9]. The strength and stiffness increases with increasing fractions of SiC, though the ductility keeps decreasing [10].

In the case of continuous fiber reinforced composites, the fibers act as the main load bearing constituent. Whereas, in the case of particulate reinforced MMC, the matrix is still the major load bearing component. The strengthening occurs mainly due to SiC particles inhibiting matrix deformation. When the reinforcing is provided by discontinuous whiskers it is a combination of both. In this case, the composite not only have better strengths than particulate reinforced composite, but, it still maintains the ease of fabrication. During processing, these whiskers become partially aligned along the rolling direction.

The stiffness of the composite can be given by a simple rule of mixtures as

$$E_c = V_m E_m + V_w E_w$$

where V is the volume fraction, E is the elastic modulus, and c,m,w stand for composite, matrix and whisker respectively. Theoretical models, based on continuum mechanics have been formulated to calculate strengthening by different fractions of SiC, either in the form of long fibers or discontinuous particulates or whiskers [11]. However they are unable to accurately predict the composite strength.

Microstructure

The main alloying elements for 6061 aluminum are 1 wt% Mg and 0.6 wt% Si. Reinforcing 6061 aluminum with 20% discontinuous SiC whisker increases the strength by 100 MPa (32%), and further substantial strengthening can be achieved by treating to a set of thermo-mechanical treatments. The same age hardening treatment, as given to 6061 Al alloy (T6) is used. The aging operation for 6061 Al alloy involves solutionizing the alloy, followed by quenching to obtain

a supersaturated solution of Si-Mg in the Al matrix. The third step involves holding the supersaturated solution at an elevated temperature (175°C) for an optimum time, for proper precipitation of the strengthening phase [12]. During aging, the transformation occurring is

$$SS \rightarrow GP zones \rightarrow \beta'(Mg_2Si) \rightarrow Mg_2Si$$

The GP zones or the β' precipitate (incoherent) is responsible for substantial strengthening. This precipitation hardening occurs due to increased energy required for the dislocations to cut through the precipitates [12].

In SiC/Al composite reinforced with discontinuous SiC whiskers, the matrix is still the main load bearing constituent. Papazian [13] carried out a detailed study on the microstructural development. He concluded that, though the overall aging sequence in SiC/Al MMC is the same as in 6061 Al, precipitation and dissolution kinetics were accelerated. Thus, the volume fraction of various phases is modified compared to the 6061 alloy. He observed that the volume fraction of the GP zones was greatly reduced.

The strength of SiC/Al was higher than the value predicted by continuum mechanics. This was due to much higher dislocation density and smaller grain size, which is due to the presence of 20 percent SiC whiskers. The grain size measured was around 2-3 microns. Dislocation density is normally on the order of 10^{14} m^{-2} [14]. The increased dislocation density is due to the large mismatch (1:10) in the thermal expansion coefficients of SiC and Al. This causes stresses during cooling which results in the increased dislocation density [15-17]. In an elegant work, Vogelsang et al [18] used insitu high resolution electron microscopy to clearly depict the generation of these dislocations at the interface due to differential thermal contraction.

SiC And Al Interface

The interface between the strengthening phase and the matrix is recognized as the single most important factor for any composite. The bond serves as a mode of load transfer between the matrix and SiC. Good bonding is essential to enable maximum loading of of SiC whiskers. A theoretical study performed by Li et al to understand the bonding mechanism, showed that its possible to have a high strength bond between SiC and Al [19].

The SiC/Al interface has been a center of much research in the last few years. So far, three theories have been proposed explaining the interface structure [20-22]. The first one claimed existence of a SiO_2 film at the interface. The second proposed Al_4C_3 between SiC and Al. The third, which has currently become the most popular, proposed that no additional phase exists between SiC and Al. This has been established using high resolution electron microscopy and Auger electron spectroscopy [23]. (Note that the processing technique can cause a significant change in the interface characteristics).

The interface characteristics or the nature of bonding plays an important role in determining the failure mode of the composite. Depending on the bond strength, fiber pull-out, interfacial debonding or whisker fracture can occur. Nutt demonstrated fracture initiated at the interface, due to very high stress concentration at the whisker end, which led to void formation and decohesion [24].

Since the interface is a region of chemical and structural transition, it may become unstable at higher temperatures, due to chemical reactions, diffusion or other changes. Chemical reaction may lead to formation of brittle intermetallic phase, which may be detrimental to the composite fracture strength. This aspect is discussed later in this section.

Thus, when we consider welding of SiC/Al composite, it becomes important to examine the changes taking place at the interface. Though the structure of the interface is now well understood, very limited data has been published about the effect of high temperatures on the interface structure.

C. Heat Flow During Welding

Rosenthal and Adams were responsible for the pioneering work to analyze the heat flow during welding and express it in terms of a simple mathematical expressions [25-26]. Over the years, these equations have been solved for various conditions. Kou [27] formed a finite element model to obtain a plot of the variations in temperature with time, experienced by a 6061 aluminum plate during fusion welding. There was very good agreement between the calculated and experimental values. Typical thermal cycles encountered during welding are shown in Figure I.

The following characteristics are observed:-

i) The peak temperatures decrease rapidly as we move away from the weld.

ii) The time required to reach the peak temperature increases with increasing distance from the weld centerline.

iii) The rate of heating and the rate of cooling both decrease with increasing distance from the weld centerline.

The temperature profile depends on heat input, as well as the material characteristics such as specific heat and conductivity, and also the plate thickness.

The changes taking place due to the thermal exposure during welding depends on the temperature profile. Thus, establishing the right thermal profile

is extremely important for the study of metallurgical changes in any heat treatable alloy.

Effect of Heat Flow on 6061 Al:

6061 aluminum alloy and SiC reinforced 6061 Al matrix composite are both used in the T6 condition, viz., solution heat treated followed by artificial aging. The effects of this treatment becomes grossly modified in the vicinity of the weld. The extent of these changes on the mechanical properties should be taken into account during its usage as a welded material [28].

The main changes taking place in the HAZ of an Al alloy structure are:-

(a) The softening (annealing) of working hardening

(b) overaging or dissolution and reprecipitation of the age-hardening precipitates

(c) recrystallization of the base material just adjacent to the weld. (Figure 2)

Away from the base plate into the HAZ, there is reversion of the metastable age-hardening phase due to thermal exposures, at the same time there is also coarsening of this phase (overaging). Still further ahead in the HAZ, there is more dissolution of β' due to exposures to higher peak temperatures. This leads to increased softening close to the fusion zone [29-31].

Some of the softening effects may be reduced due to post weld aging. In the region just adjacent to the fusion zone, there was complete dissolution of the precipitates during heating, some of which reprecipitates on holding at room temperature (natural aging). This can be enhanced by aging at higher temperature (artificial aging) as shown in Figure 3. But further away from this region, there is overaging, which does not respond to post weld aging.

Effects on SiC/Al

In 20v% SiC/6061 Al composite, it is a somewhat similar situation in the matrix, though a few more factors come into play. SiC presence causes an increased dislocation density and much smaller grain size. This leads to an enhancement of the dissolution and precipitation rates [13]. High temperatures may also cause porosity due to evolution of hydrogen, which usually gets entrapped during processing.

The most crucial factor to be taken into consideration is the modification of the interface due to the existence of interfacial reactions. The reaction between SiC and Al is

$$3SiC(s) + 4Al(l) = Al_4C_3(s) + 3Si(s)$$

Iseki [21] studied the thermodynamics of this reaction at various free Si concentrations. The Al-SiC system is quite stable until we reach the liquidus temperature of Al. The expression for the free energy change of this reaction is

$$\Delta G(J/mol) = 113900 - 12.06T\times \ln T + 8.92\times 10^{-3}T^2 + 7.53\times 10^{-4}T^{-1} + 21.5T + 3RT\ln a_{[Si]}$$

The free energy change becomes more and more negative with increasing temperatures, and the reaction can proceed spontaneously.

It is necessary to consider the kinetics of this reaction, which would be governed by the activities of C and Si in molten aluminum. The stability of Al-C-Si system at various temperatures, in terms of C activity in Al is given in Figure 4 [32]. The bold line separates the stable phases in Al-C system in terms of C activity. Similarly, the dashed line separates the Si-C system into stable domains at different temperatures. Note that, unlike Al, Si remains in solid state

throughout the temperature range into consideration.

SiC can dissociate to Si and C, thereby increasing their activities in aluminum. Once the activities of Si and C reach their respective solubility limits, they start precipitating as free Si and Al_4C_3, as indicated in Figure 4. Also, the domain of of stable SiC gets reduced if the activity of dissolved Si is less than solid Si phase (shown by dotted lines in the figure). Thus it gets easier to reduce SiC at very low Si activity. Hence, it is advantageous to use 6061 Al as matrix, due to its Si content instead of pure Al, so as to decrease the chances of aluminum carbide formation. Thermodynamics considerations have shown that Al_4C_3 may not always be one of the reaction products. It is precipitated only when the solubility limit of carbon in molten Al is exceeded The reaction however modifies SiC surfaces due to Si precipitation at the interface.

The formation of aluminum carbide degrades the bonding between SiC and Al matrix, which reduces mechanical properties It also lowers the fluidity of the melt, which is undesirable during welding. Hence it becomes important to check the extent of interfacial reaction. Recently, two novel techniques have been reported for studying the extent of this reaction [33,34]. The first technique involves measuring the change in the matrix liquidus temperature, which changes due to Si formation which is one of the reaction product. The second technique uses TEM to analyze the reaction products.

D. Welding of SiC/Al

Very limited data has been published regarding the fusion welding of SiC/Al metal matrix composite. The problems encountered during welding are, porosity due to evolution of hydrogen, poor fluidity of the melt, and above all, the formation of aluminum carbide which degrades the mechanical properties and corrosion resistance.

Ahearn et al [35] reported the first attempt of fusion welding SiC/Al. Porosity was greatly reduced by vacuum degassing the plate before welding. Due to presence of 20 percent SiC, fluidity of the composite is very poor. Hence various Al alloys, such as 4043 and 5356 were used as filler wires. Welds made by gas tungsten arc welding (GTAW) process were of poor quality due to relatively higher heat inputs. Using gas metal arc welding (GMAW) process, it was possible to make sound welds. Some of them failed in the HAZ during tensile testing. Subsequent age-hardening improved the strength considerably. There are also a few references of structurally sound welds produced by GTAW process and using aluminum alloys as filler metal. But, much of this data has not been published due to strategic importance of this material for defense purposes [29].

Capacitor discharge has also been used successfully to join SiC/Al. This technique circumvents porosity, fluidity and Al_4C_3 problems [36]. But it is restricted to small cross-sections only, which could be a limitation to many of the structural applications. It has been shown that very high energy inputs during GTAW or laser welding produces large amounts of brittle aluminum carbide [38-39]. Recently excellent joint efficiencies have been reported by using inertia welding and brazing [37].

Summarizing, SiC reinforced 6061 Al matrix composite has been found to have excellent properties which makes it very desirable for various structural applications. Also in the last few years considerable insight has been gained about its microstructure and the interface structure. But, much work still remains to be done regarding its response to thermal exposure during welding, changes in matrix structure and properties in the HAZ, and changes at the interface due to interfacial reaction. This is essential for further advancing the welding technology for SiC/Al composites, an important aspect for structural fabrication.

III. Experimental Procedure

A. Materials

6061 aluminum matrix reinforced with 20 volume percent discontinuous SiC whiskers composite, in the T6 condition, was supplied by DWA corporation. It was obtained in the form of 3.2mm plate. The 6061 aluminum alloy was also in the form of 3.2mm plate in the T6 condition.

B. Specimen Preparation

The specimens were machined as shown in Figure 5, for gleeble studies. The generation of microstructure similar to each sub-zone in the HAZ, requires a very carefully selected specimen geometry. The zone of interest (work zone) is obtained at the center of the specimen. The specimen was subsequently, mechanically tested. Keeping this in mind, the geometry of the specimens chosen is shown in Figure 5. The reason for this geometry was to obtain a large work zone with negligible thermal gradients. Thus the specimens had to be at least 15 cm long. This was essential for the mechanical tests and to insure that the fracture took place in the work zone at the specimen center. This was guaranteed by reducing the width in the center of the specimen. The radius R of the fillet was chosen by trail and error. A smaller radius caused the fracture to occur at the edge of the gage length due to stress concentration, and due to the fact that SiC/Al composite is very brittle. Finally, a 19 mm (0.75 inch) tool was selected

for milling the gage length and this also corresponds to the radius of the fillet.

Also, with this particular geometry of the specimens, higher temperature gradients due to the changing specimen width just away from the center, results in higher cooling rates in the work zone. Thus, cooling rates are closer to the actual welding condition. A specimen with a constant width would not have provided us with this advantage.

C. Thermal Cycling

The thermal cycles experienced during welding, were simulated on a gleeble interfaced to a personal computer. The desired thermal cycle, namely, the heating rate, the peak temperature and the cooling rate were input into a program which controlled as well recorded the thermal cycle. The controlling software was calibrated to match the thermal characteristics of the material. Since the thermal conductivity and specific heat of both the composite and the unreinforced alloy were almost same, (Table I) their thermal responses were similar.

The specimen was fixed between the jaws on the gleeble, which serve for conducting heat as well as current. The specimen is resistance heated by passing current through it depending on the desired thermal cycle. At the same time, it is cooled continuously at the ends. Also the heat and current flow is along the axial direction only, thus, planes normal to the axis are virtually isothermal. A chromel-alumel thermocouple was spot welded at the center of the gage length (Figure 6). The temperature is continuously monitored in this region, the work zone, or the region experiencing the desired thermal cycle. Different peak temperatures were chosen to reproduce the entire length of the HAZ. The cooling

rates corresponding to different peak temperatures in the HAZ were of little relevance in this study. The thermal cycle experienced (Figure 7) compared well to that experienced during actual welding [27], the cooling rates were lower. Exactly the same treatments were also given to 6061 Al alloy. Also one of the specimens was held at 525°C for one hour. The reason for this is discussed later. Subsequently, the thermocouples were detached from the specimens and the specimens were given final milling and polishing, to remove any marks due to the spot weld.

To study fusion zone changes, specimens were heated in a furnace to various temperatures, above the liquidus temperature of 6061 Al, 652°C. The specimens were held at the peak temperature for 15 minutes, a very long time compared to actual zones which experience such peak temperatures only momentarily. The main idea was to enhance whatever changes that took place. This does gives a good qualitative picture of the changes undergone.

D. Mechanical Testing

After giving the requisite thermal cycle for simulating weld induced changes, the specimens were subjected to tensile testing on Instron (model 1335). A constant ramp load was applied. Plots of load vs displacement were obtained (Figure 8) which were used to calculate strengths and percent elongation. Hardness measurements were made on the Rockwell hardness tester. The Rockwell scale 'B' was used.

The tensile tests were carried out within 24 hours after the thermal cycling, thus giving very little time for natural aging.

E. Metallography and Fractography

One set of specimens was used only to study the changes in the microstructure. After giving the thermal cycle, transverse sections were made in the work region, and the specimens were polished to a 1 micron diamond finish. 5 ml HF, 10 ml H_2SO_4 and 85 ml water was used as an etchant for 6061 alloy grain boundary outlining. Kellers reagent was used for highlighting the precipitates . The composite specimens observed under the scanning electron microscope (SEM) were heavily etched with HCl.

Fracture surface analysis was carried out on JSM-35 SEM. An accelerating voltage of 25 kV was used. Energy Dispersive X-rays analysis was also carried out to detect changes due to high temperature treatment.

F. Transmission Electron Microscopy

The specimen was first ground to about 125 microns thin foil. 3mm disks were punched out of this foil. These disks were further carefully ground to about 25-30 microns. Subsequent thinning to perforation was done using ion mill. Transmission electron microscopy (TEM) was performed on Hitachi H-800 STEM at 200 kV.

IV. Results

A. Base Material Properties

The effect of 20% SiC reinforcement on 6061 aluminum alloy is seen in the plot of the tensile test, carried out at room temperature for the as-received material (Figure 8). On measuring the strengths and percent elongation it is observed that:-

(i) The ultimate tensile strength improved from 262 MNm^{-2} (38 ksi) to 490 MNm^{-2} (71 ksi), and the yield strength improved from 241 MNm^{-2} (35 ksi) to about 434 MNm^{-2} (63 ksi). For the composite, the ultimate tensile strength was same as the breaking stress.

(ii) The composite was very brittle compared to the unreinforced Al alloy. Unlike 6061 Al there was no necking before fracture. The percentage elongation to failure was just a small fraction of that of 6061 Al.

(iii) The modulus of elasticity improved from 69 GPa to 106 GPa [10] which is demonstrated by the increased slope of the composite over 6061 Al.

Thus, reinforcing 6061 Al with SiC considerably improved the hardness, strength and stiffness, but caused a substantial drop in the ductility. Also, the composite maintained its much superior strength after various high temperature thermal cycles.

B. The Simulated HAZ

Thermal cycling caused softening in the simulated heat affected zone, for both unreinforced and reinforced Al alloy. The response of the mechanical properties to various peak temperatures experienced in the simulated HAZ are presented in Figures 9-12. This gives the extent of softening in the entire HAZ. The softening increases with increasing peak temperature, which corresponds to decreasing distance from the fusion zone. The changes in each of the property are discussed below.

Yield Strength

The variation in the yield strength (YS), corresponding to the different regions of the HAZ, (experiencing different peak temperatures), is plotted in Figure 9. Though the composite showed a drop in the yield strength, it maintained its much superior strength as compared to the unreinforced alloy. The drop in the YS in the HAZ for SiC/Al composite was from 448 MNm^{-2} (65 ksi) to 262 MNm^{-2} (38 ksi), compared to a drop from 207 MNm^{-2} (30) ksi to 62 MNm^{-2} (9 ksi) for 6061 Al. SiC/Al composite showed more significant YS reductions at the lower temperatures than did the 6061 alloy. The biggest drop in the YS took place in 250-350 °C range, compared to 350-500 °C range for 6061 Al. SiC/Al, in fact, showed a slight increase in YS above 500°C. The specimen held at 525°C for one hour showed no decrease in the YS, compared to the one which experience the same temperature only momentarily (in the HAZ).

Ultimate Tensile Strength

In the case of SiC/Al, the ultimate tensile strength (UTS) was the same as the breaking stress, due to very low ductility. The drop in the UTS for both the composite and 6061 Al was smaller than observed for the drop in the yield strength (Figure 10). In the HAZ, the UTS of SiC/Al dropped from 489 MNm^{-2} (71 ksi) to 400 MNm^{-2} (58 ksi). 6061 aluminum exhibited a drop from 255 MNm^{-2} (37 ksi) in the base material to 186 MNm^{-2} (27) near the fusion zone. Thus, the strength of the composite in the HAZ, even very near the fusion zone, was much higher than that of the unreinforced alloy at room temperature. The largest drop in the UTS for the composite took place in the 250-300 °C range. There was a negligible drop beyond 350 °C. In the case of 6061 Al, there was a uniform drop extending over the entire simulated HAZ.

Ductility

The presence of 20 percent SiC whiskers caused a substantial difference between the percentage elongation values for SiC/Al and 6061 Al (Figure 11). The unreinforced alloy underwent necking before fracturing, which was totally absent in the composite. For 6061 Al, the HAZ percent elongation value increased from 26% to 42% as a function of increasing peak temperatures. On the other hand, SiC/Al showed a very modest increase even in the specimen exposed to a HAZ peak temperature of 550 °C.

Hardness

The presence of hard SiC whiskers significantly increased the hardness of 6061 Al The trend of reduced hardness in the simulated HAZ for SiC/Al, was

somewhat similar to the trend for YS (Figure 12). The hardness dropped from a maximum value of 78 HB in the T6 condition, to 60 HB, near the fusion zone. Maximum lowering occurred in the 250-350 °C range. Beyond 400 °C there was a negligible drop, and above 500°C a slight increase was observed.

Microstructure

Figure 13 compares the microstructures of the as received 6061 Al to the one exposed to 500°C peak temperature. The long elongated grains were recrystallized due to thermal exposure in the simulated HAZ, at the peak temperature of 500°C, which is close to the fusion zone. The specimen subjected to a peak temperature 500 °C showed large, nearly equiaxed grains. There was also reversion of the age-hardening precipitate, which cannot be resolved under the optical microscope. These Mg-Si precipitates are on the order of a few nanometers.

The SiC whiskers had aspect ratios, viz., the ratio of length to diameter, from 2-10 (Figure 14). Most of the whiskers were in general aligned parallel to the plate surfaces due to rolling. There was also some whisker breakage taking place during rolling. Thermal exposures in the simulated HAZ, resulted no detectable change either in the distribution or the morphology of SiC, or the matrix, or the interface, as observed under the optical microscope. No reaction took place between SiC and Al after holding the specimen at 525 °C for one hour. For the same specimen, the mechanical properties and the microstructure were found to be similar to specimen experiencing the same peak temperature only momentarily, as in the HAZ.

Fractography

6061 Al showed considerable plastic deformation before fracturing. The fractographs are full of large dimples (Figure 15) indicating a very ductile fracture.

SiC/Al composite exhibited very little elongation to failure. Observing the fractographs of the specimen in the T6 condition, showed some dimples, which were fewer and much smaller than those observed the 6061 alloy [16]. At higher magnification, each of the dimples was full of micro-dimples, and very little SiC was visible on the surface. The fractographs of the specimen which was exposed to 500°C was quite similar, though the surface was more uneven with more and larger dimples (Figure 17).

C. The Simulated Fusion Zone

The MMC was held at various temperatures above the liquidus temperature of 6061 Al, for 15 minutes in order to increase the severity of the changes taking place. The most obvious change taking place was the formation of porosity (Figure 18). This was mainly due to the evolution of gases like hydrogen which are entrapped during powder processing. On exposure to high temperature, the gases evolved leaving behind large porosity. It was detected only in the specimens exposed to temperatures 750 °C and above. The extent of porosity was very severe at 850 °C and above. Some of the pores were large enough to be observed with with naked eye.

Another significant change observed in the optical micrographs was the formation of a new grey colored phase, present mainly around SiC (Figure 19). This implied the occurrence of an interfacial reaction between the SiC and the

aluminum matrix. The proportion of this grey region increased with increasing temperatures. Observation of the same specimen under the SEM showed the presence Si uniformly distributed throughout the microstructure, which was confirmed using energy dispersive X-rays analysis (Figure 20). No aluminum carbide could be detected under the optical microscope in spite of the presence of substantial amounts of free Si.

D. TEM analysis

The TEM specimens were all taken along a longitudinal section. Most of the whiskers were parallel to the specimen plane. The SiC whiskers were around 0.3-0.4 microns in diameter, and the length was in the 2-10 micron range. Note that much of the whiskers break during fabrication.

SiC whiskers were mainly in the form of β-SiC, which has a cubic structure. They have a hexagonal cross-section. The micrograph (Figure 21) showed a large number of bright and dark fringes in SiC, along planes perpendicular to the whisker axis. The whiskers were grown in [111] direction, and many planar defects result on the close packed planes. These defects are mainly micro-twins which caused streaking in the [110] pattern.

Good wetting was observed between the SiC whiskers and the Al matrix. The matrix of the as-received composite in the T6 condition was highly dislocated with the tangled dislocations extending throughout the matrix (Figure 22). The dislocations were decorated with age-hardening precipitates. The matrix at the interface between SiC and aluminum was again very heavily dislocated. In the as received specimen, no additional phase was seen at the interface. There

was a direct transition from SiC to aluminum (Figure 23)

The specimen held at 1100°C , still showed little change in SiC morphology and the matrix was still very heavily dislocated, though slightly less than the untreated specimen (Figure 24). The SiC interface had clearly undergone a change as compared to the as-received composite. Interfacial reaction was obvious due to the presence of a new high contrast material, determined to be silicon (Figure 25). Energy dispersive X-ray analysis (EDX) on the STEM at various points along a line extending from SiC whisker to well within the matrix, revealed that the Si fraction had increased considerably in the matrix around the interface. Si, formed at the interface, had diffused into the matrix. The extent of Si formation and diffusion into the matrix is shown in the EDX plot.

V. Discussion

The results presented in the previous section are systematically analyzed in this section. The mechanical properties and the structure of the base material are considered first. The changes in the base material due to thermal exposure in the HAZ are discussed subsequently. This is followed by an analysis of the simulated fusion zone structure on the basis of optical, SEM and TEM micrographs.

A. Base material

Reinforcing 6061 aluminum with high strength, high stiffness discontinuous SiC whiskers leads to changes in the matrix microstructure. The grain size is much smaller than the unreinforced alloy, and also, the dislocation density is much higher. This leads to a substantial increase in the strength and hardness values. The increase in the yield strength (120%) is much larger than the increase in the UTS (80%). The substantial increase in stiffness is also very desirable for most applications. Thus, the matrix microstructure is a significant factor determining the properties of the composite. But the increase in hardness, strength and stiffness value is accompanied by a substantial decrease in tensile ductility and fracture properties. This could be a limitation in many applications.

B. The Simulated HAZ

6061 Al alloy

Thermal processing is mainly responsible for strengthening of 6061 Al alloy. The microstructure of the base material in the T6 condition is characterized by the presence of β' age hardening precipitate throughout the matrix. In the heat affected zone, there is a reversion of these effects to various degrees depending upon the distance from the weld centerline.

High temperatures cause annealing in the form of recovery and recrystallization of the stressed grains. The strained elongated grains tend to become stress-free and recrystallize as fresh equiaxed grains. The extent of recrystallization increases with increasing temperatures and time. This causes drop in the YS. Thus, as the peak temperature increases, the strength values decrease, and there is an increase in ductility. Also, there is a probable change in the age-hardening phase β'. The precipitate starts undergoing dissolution at the same time some of them start coarsening. The dissolution of β' starts around 250–300°C. Thus, there is an increased rate of the drop in the YS for the 6061 Al in this range, and an increase in the percent elongation.

At temperatures above 500°C, there is complete dissolution of β', hence no further change in the YS. In fact, exposing the alloy at this temperature and above would cause a slight increase in the room temperature YS and hardness, due to natural aging in this region. But in the region experiencing peak temperatures in the 150–450°C range, there is no natural aging because most of the precipitate is in the form of coarse β precipitate. The only way to revert back hardness in this region is by solutionizing again followed by age hardening.

An important point to note here is that the drop in the UTS is much less than the corresponding drop in the YS. YS is dependent on the movement of dislocations, which is considerably modified due to presence of age-hardening precipitates. This shows that the yield strength is more sensitive to the thermal and mechanical processing than the UTS.

SiC/Al composite

In the simulated HAZ, the yield strength starts decreasing at lower peak temperatures than in the 6061 Al alloy. Also, unlike 6061 alloy, the drop is larger in the lower temperature ranges then at higher temperatures. This can be explained on the basis of microstructure. The tangled dislocations in the matrix act as nucleation sites for age-hardening precipitates. This leads to an increased rate of precipitation as well as dissolution. The dislocations probably act as high mobility paths for Si and Mg atoms, thus increasing the diffusion rates. The biggest drop in the YS for SiC/Al takes place in the 250–300°C range, when there is believed to be complete dissolution of the β' precipitates. The mobility of the dislocations is directly dependent on the fraction and the form of these precipitates, which essentially act as barrier to the their movement. Thus, dissolution of β' leads to a rapid drop in the dislocation density and thus more softening.

Other than work-hardening, another important source of dislocations in SiC/Al composite is the mismatch in the thermal expansion coefficients of the composite and Al alloy. On cooling after exposure to any high temperature, there is a build up of stresses at the interface which leads to re-emergence of dislocations. Thus, even on exposure to very high temperature, the matrix still has a very high dislocation density. This is shown in the TEM of the specimen exposed

to 1100°C for 15 minutes (Figure 24).

After exposure to peak temperature of 350°C, the simulated HAZ specimens showed very little fall in the YS. Above 450°C there was a slight increase in YS. This is most likely due to natural aging, which was again higher than in 6061 Al, due to increased precipitation rate in the matrix of SiCAl composite.

Optical microscopy showed no change in the microstructure of the simulated HAZ. There was no change in the SiC morphology, nor any sign of any interfacial reaction between SiC and aluminum. Thus dissolution and coarsening of the age hardening precipitate are the only responses to the thermal exposure in the HAZ. This was confirmed by holding one of the specimens at 525°C for one hour. The specimen showed no additional reduction of strength or hardness, than what had already been achieved by exposing to the same peak temperature only momentarily, as in the HAZ. Had there been any reaction between SiC and Al, it would have resulted in further decaying of the properties with temperature.

Comparing the fractographs of the composites, the one exposed to a peak temperature of 500°C, showed an increase in the size of the dimples over the specimen in the T6 condition (at low magnification). But the dimples are much smaller than the 6061 Al alloy. In the higher magnification fractographs, the negligible amount of SiC visible on the surface indicates that the fracture proceeds mainly through the matrix, without fracturing most of the SiC whiskers. Instead the whiskers just separate from the matrix, which causes the appearance of the micro-dimples which are seen in the high magnification fractographs.

C. The Fusion zone

The specimens were held at various peak temperatures above the liquidus temperature of 6061 Al, for 15 minutes which is a very long time compared to that experienced only momentarily in the actual fusion zone of a weld. This will enchance the severity of changes taking place in the fusion zone at similar temperatures.

The most obvious development on exposing to high temperature was the presence of large amounts of porosity. There was negligible porosity until 750°C, but above 800°C the entire specimen was full of large pores which were even visible with naked eye. Similar volumes of pores were observed in GTA welds reported by Devletian [36]. This is due to evolution of gases, mainly hydrogen, which are entrapped during fabrication. The amount of porosity can be lowered by vacuum degassing the composite and by improving the fabrication technology [35].

Interfacial reaction was evident in the optical micrographs of the specimens which were exposed to temperatures above 750°C. Si was the reaction product, present around SiC through out the specimen. The free energy of the reaction

$$4Al_{(l)} + 3SiC = Al_4C_3 + 3Si_{(s)}$$

is around -50 Joule/mole for 6061 Al alloy, at the liquidus temperature. Thus. the reaction can take place spontaneously at this temperature. However, detectable amount of precipitation of reaction products takes place only above 750°C. Si precipitation could be observed around SiC whiskers. Al_4C_3 was not detected by optical microscopy, contrary to the above equation and the reports in the

literature of existence of large amounts of Al_4C_3 precipitates due to high energy inputs during laser and gas metal arc welding [38,39].

The absence of aluminum carbide in this study can be explained on the basis of Figure 4. Firstly, the maximum temperature considered in this study is 1100°C, which is much less than the peak temperatures encountered during laser welding. At lower temperatures, SiC has a much larger stable domain than at higher temperatures. Also, the 6061 aluminum matrix has around 0.6-1.0 percent Si, and no carbon. The activity of dissolved Si is order of magnitude higher than the activity of C in Al. Thus, as SiC dissociates at high temperatures, the activities of Si and C in molten Al starts increasing. The solubility limit of Si is soon exceeded and thus Si starts precipitating. Whereas, the activity of dissolved C is still much lower than its limit, hence there is no precipitation of C in the form of Al_4C_3. It would start precipitating at some temperature higher than 1100°C, when the reaction has proceeded much further.

Transmission electron microscopy provided considerable insight into the microstructure and the interfacial characteristics. Surprisingly, the entire matrix, in addition to the region surrounding the SiC, was covered with dislocations, though relatively less dense than the specimen in the T6 condition.

The TEM micrograph of the specimen exposed to 1100°C showed the interface degraded, and the presence of Si at the interface and in the surrounding matrix. The presence of free Si as a result of interfacial reaction, may lead to to a substantial changes in the properties. Since the interface not only serves as a mode for load transfer between SiC and the matrix, but is also a site for fracture initiation, and this may cause a substantial lowering in the breaking stress

values.

D. Summary

To summarize the effects due to heat flow during simulated welding of 20 volume percent SiC whisker reinforced 6061 aluminum composite the following conclusions can be made:

(1) The extent of softening in the HAZ in SiC/Al composite is almost same as in unreinforced 6061 alloy. But the composite maintains its much superior strength over 6061 Al throughout the HAZ.

(2) No interfacial reaction was observed between SiC and Al in the entire HAZ. Thus, the softening of the composite is caused only due to annealing and removal of the age-hardened microstructure.

(3) The matrix of SiC/Al composite is very heavily dislocated, with very little change in the dislocation density throughout the simulated HAZ. This high dislocation density leads to an acceleration in the age-hardening process.

(4) The interfacial reaction between SiC and 6061 Al matrix can take place at any temperature above the liquidus temperature of 6061 alloy. But Si starts showing up only above 750°C (after holding for 15 min.). Si is formed at the interface and starts diffusing into the matrix. There was negligible precipitation of Al_4C_3, even in specimens exposed to 1100°C peak temperature.

(5) Porosity is also present in the composite after exposure to temperatures above 750°C.

(6) In the SiC/Al composite, most of the dislocations, which are annealed out during heating, are regenerated during cooling due to differential thermal contraction. Thus, the matrix always maintains its very high dislocation density.

(7) Microstructural changes in the HAZ, during welding of SiC/Al composite, may be reversed by using post-weld treatments similar to the one used for 6061 alloy. Thus, reducing heat input during welding may lead to better properties in the fusion zone, due to reduced porosity and interfacial reaction.

VI. Future Work

Minimizing heat input during welding has been recognized as one of the most important criteria for welding SiC/Al composite. Also, making the composite more heat resistant would be very desirable during welding.

One of the most promising ways to improve the limits of heat resistance of this composite, is by coating SiC whiskers with an appropriate material, which would act as a barrier to the interfacial reaction. Recently, Nathan [32] evaluated different coatings on SiC for this purpose. SiO_2 and Al_2O_3 coatings were observed to be an effective barrier to the interfacial reaction. A comparative study on the interfacial strengths of these coatings can provide with some really important results, and may thus lead to considerably more heat resistant SiC/Al composites.

The other alternative which is currently being tried out by researchers today, is by reducing heat input for making structurally sound welds. The technique involves using relatively low melting aluminum alloy such as 4043, 5356 alloys as filler wire, and thus causing as little melting of the composites as possible. This circumvents problems like porosity, interfacial reaction and low fluidity of the composite [29,37]. In this case, however, the strength of the weld will be determined by the weldmetal, whose strength might not match up to the base material strength. Welds have been made using GMAW, GTAW and inertia welding with reasonable success.

Finally, it can be said that welding technology for SiC/Al composite is still evolving. Currently, the data base is surprisingly small considering the popularity of this composite. Much more research emphasis is necessary is this area to make this composite really successful as a structural material.

Table I

Properties of 20% SiC/6061 Al composite

Properties	20% SiC/6061 Al (T6)	6061 Al (T6)
UTS, (MNm^{-2})	551.7	306.4
YS, (MNm^{-2})	448.2	204.8
Youngs Modulus (GNm^{-2})	119.3	71
% Elongation	1.4	25
Density (g/cc)	2.79	2.70
Coeff. of Thermal expansion	14.8×10^{-6}	24.0×10^{-6}
Specific Heat (J/g.K)	0.839	0.896
Thermal Conductivity (W/m.K)	143	167

(Reference 5,10)

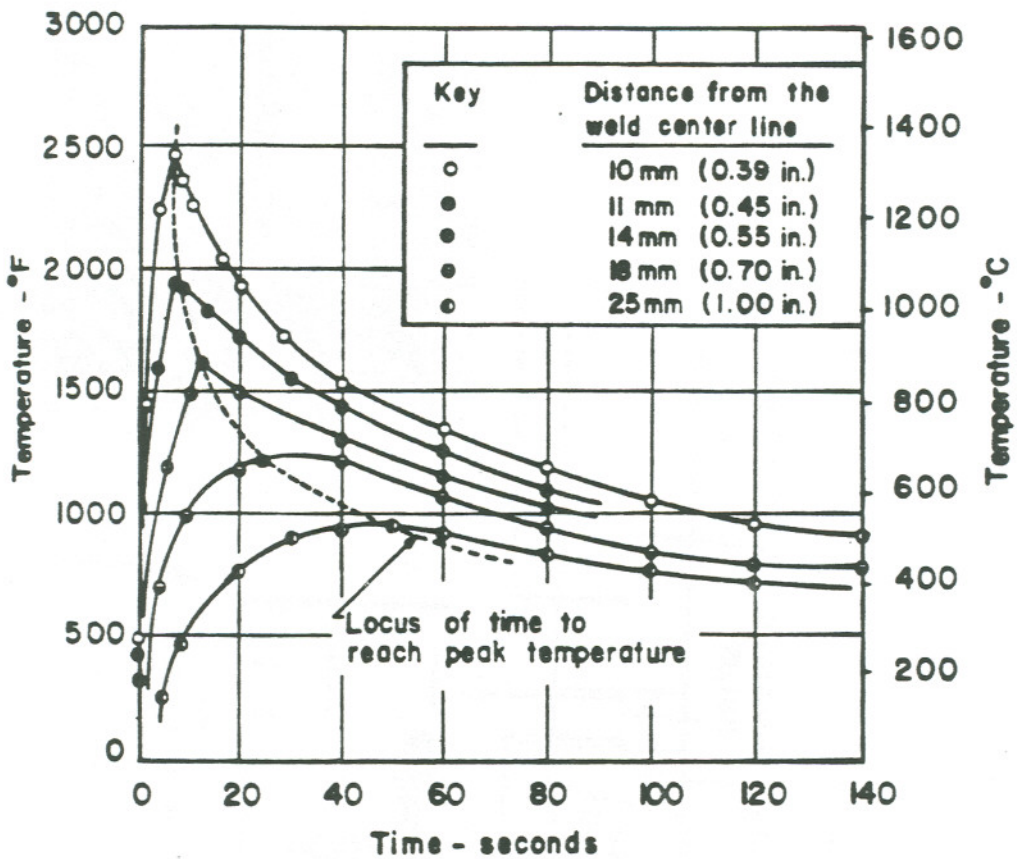

FIGURE 1 Typical thermal cycles experienced in the HAZ during fusion welding (Ref. 26)

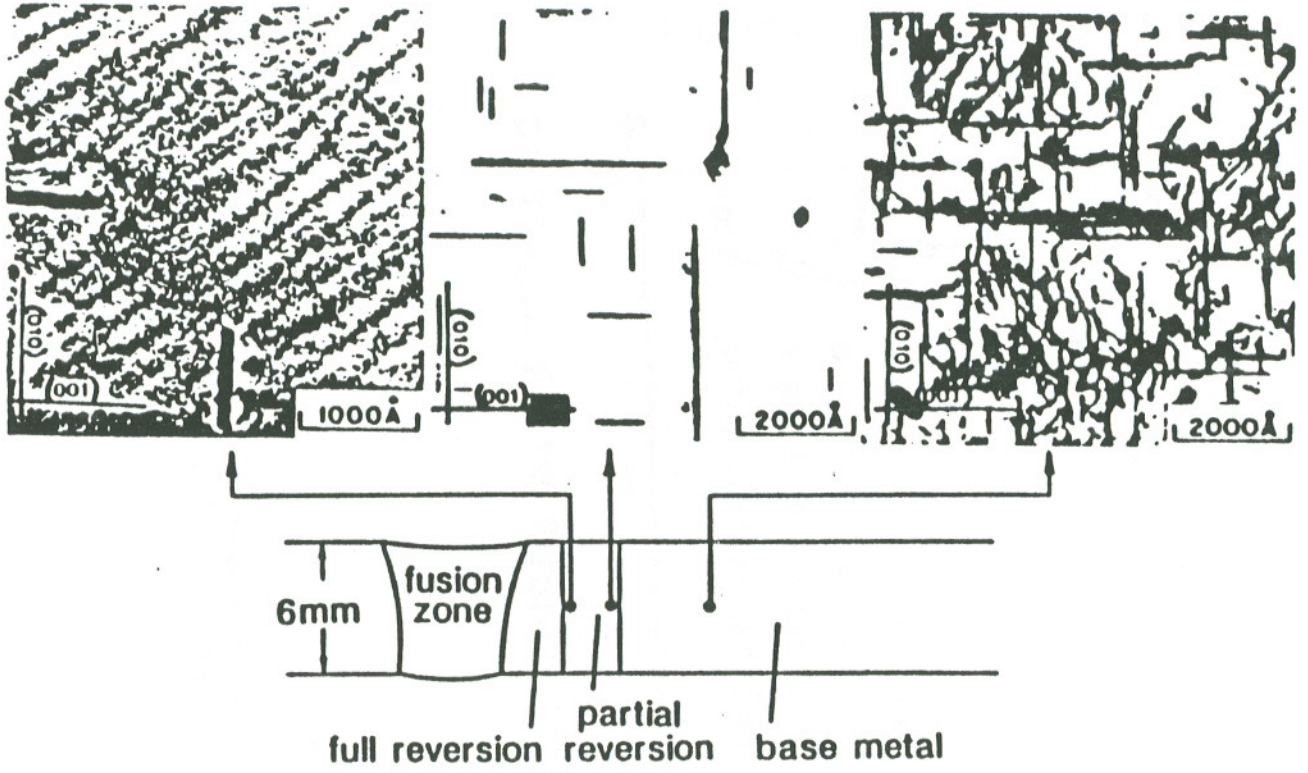

FIGURE 2. **Dissolution and Coarsening of precipitates in the heat affected zone in the age hardened Aluminum Alloy (Ref. 28)**

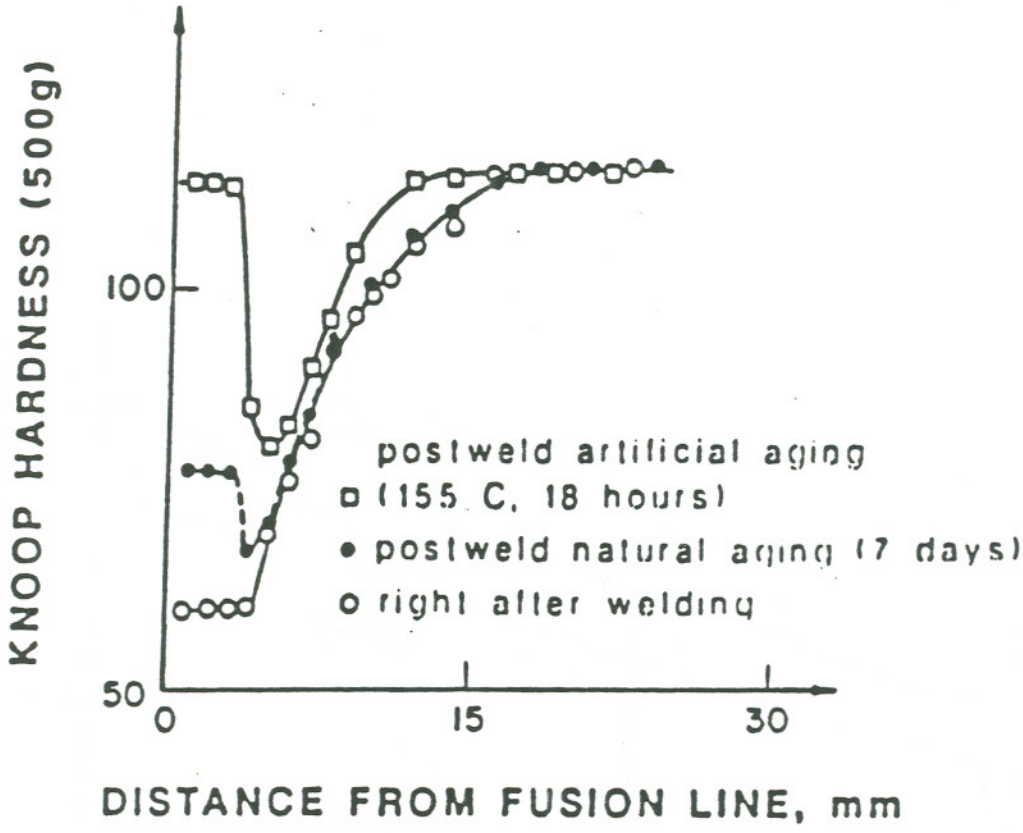

FIGURE 3. Hardness profiles of the HAZ of a GTA weld on on a 3.2 mm thick sheet of 6061 Al (T6) (Ref. 28)

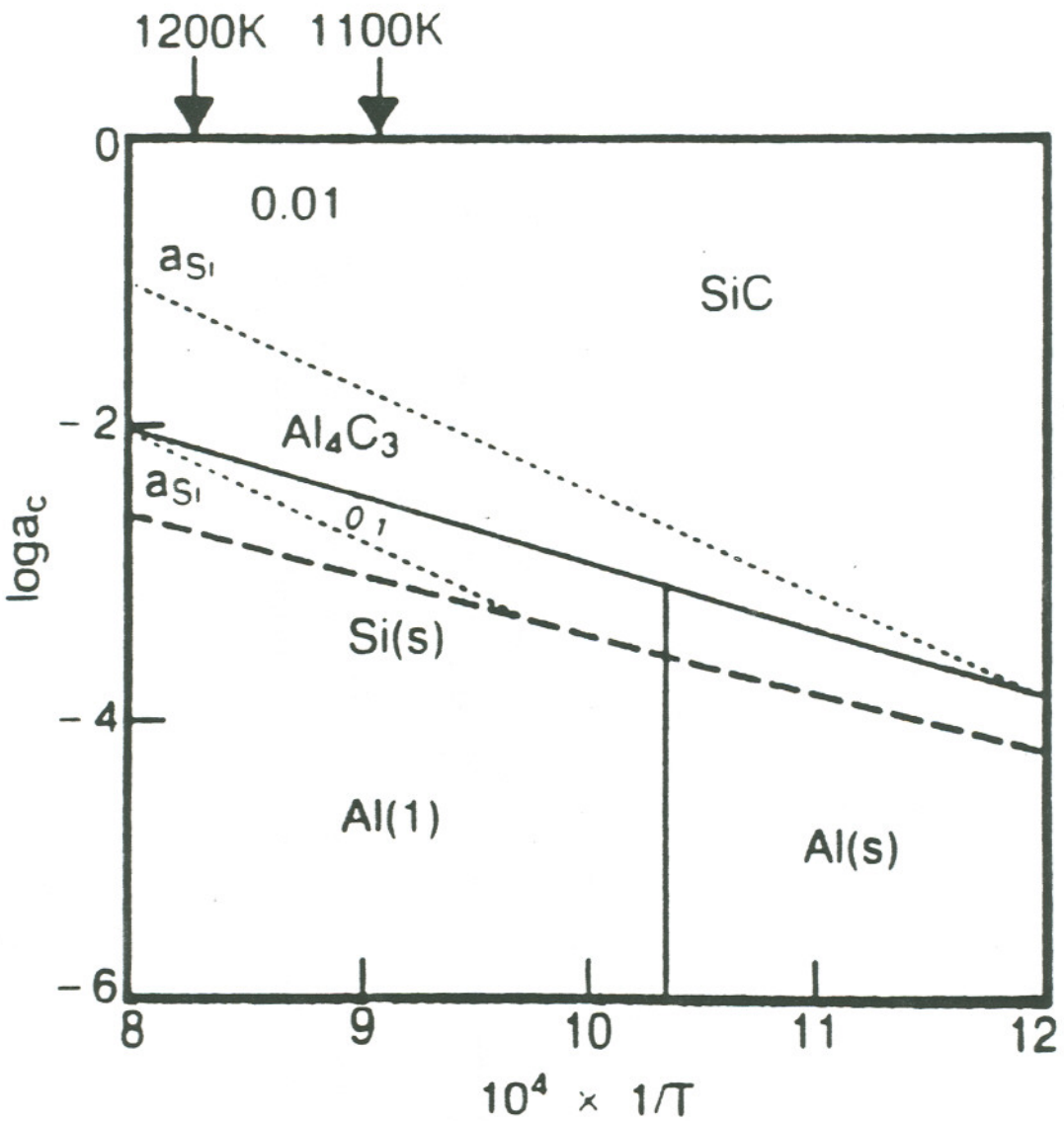

FIGURE 4. The stability domain diagram for Al-C-Si system (Ref. 32)

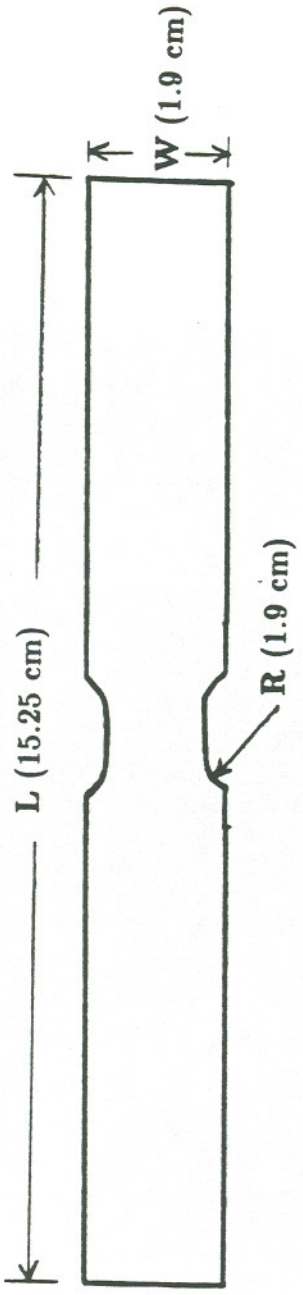

FIGURE 5. Geometry of the specimen

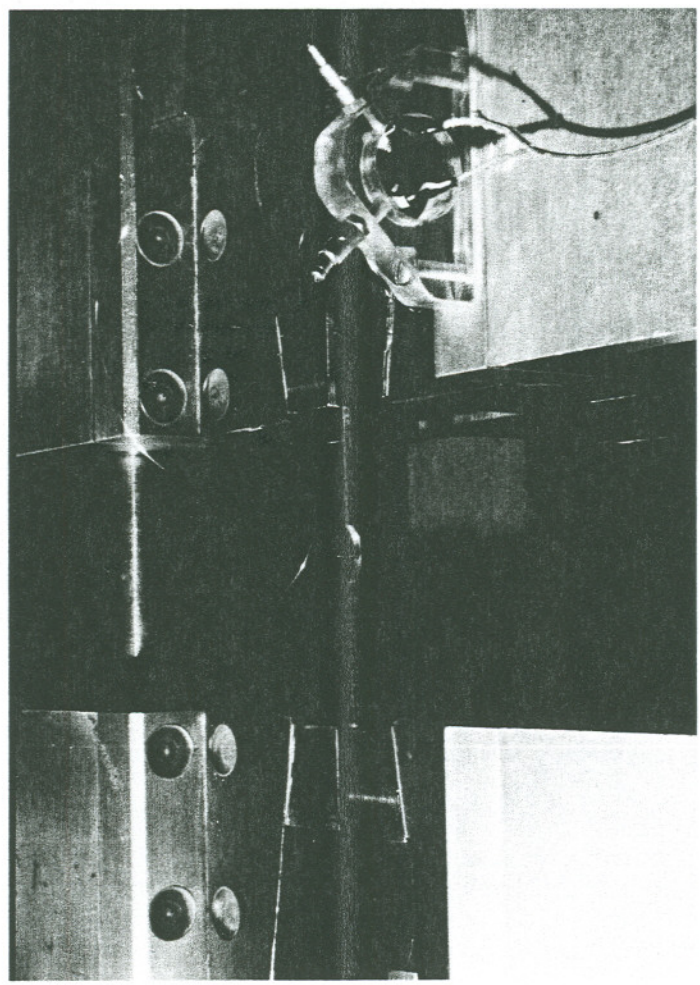

FIGURE 6 The specimen mounted on the Gleeble

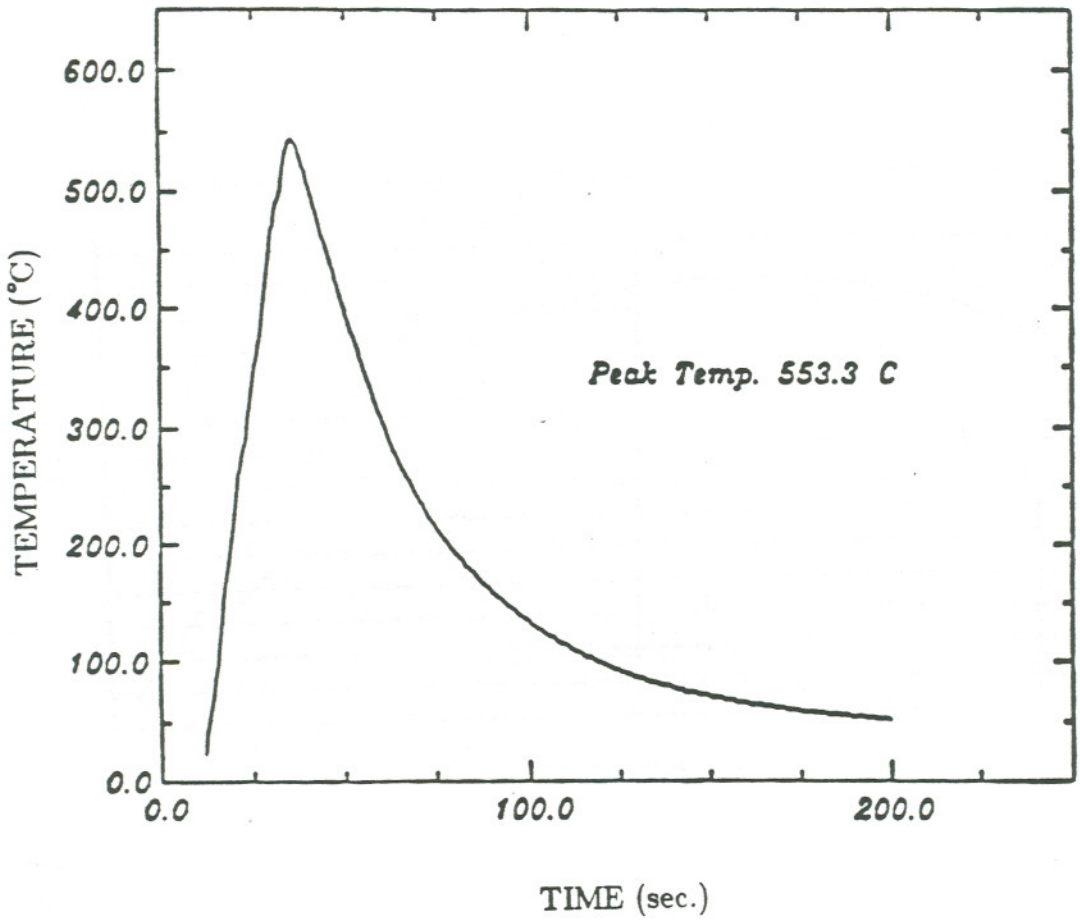

FIGURE 7. **Typical thermal cycle produced using the Gleeble**

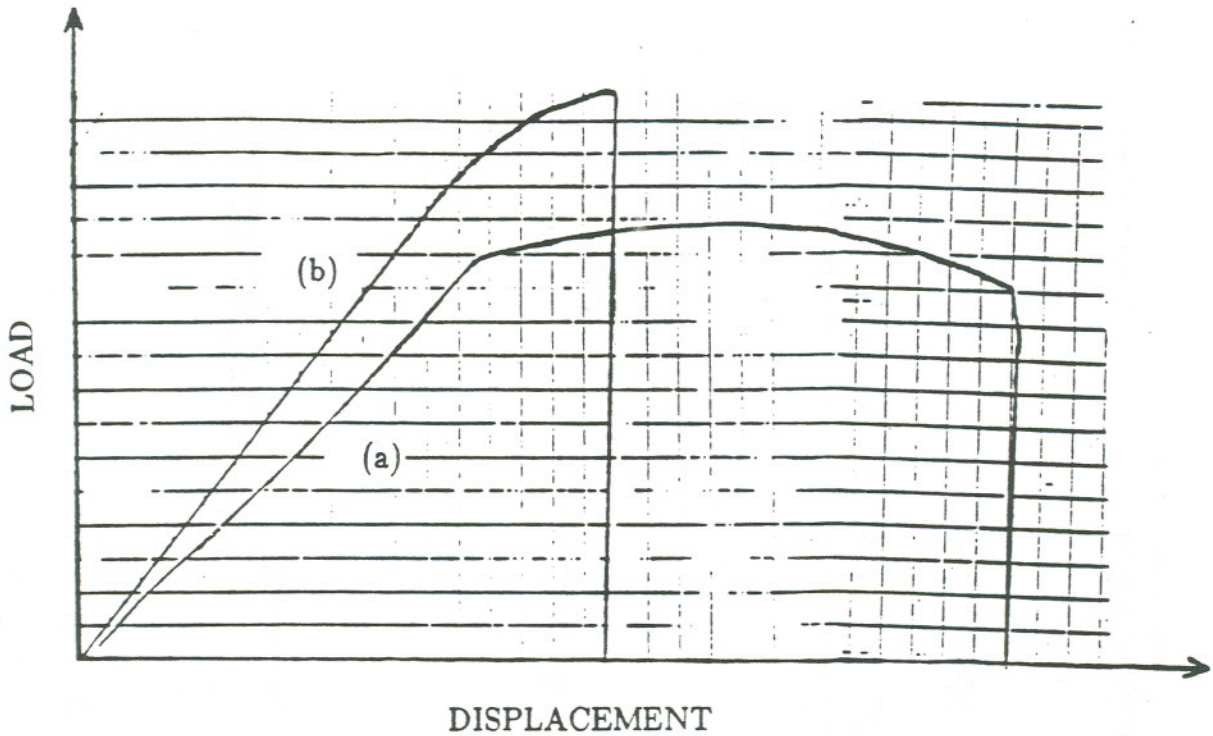

FIGURE 8 **Typical load vs displacement plots for (a) 6061 Al, (b) 6061 Al reinforced with 20% SiC discontinuous whiskers**

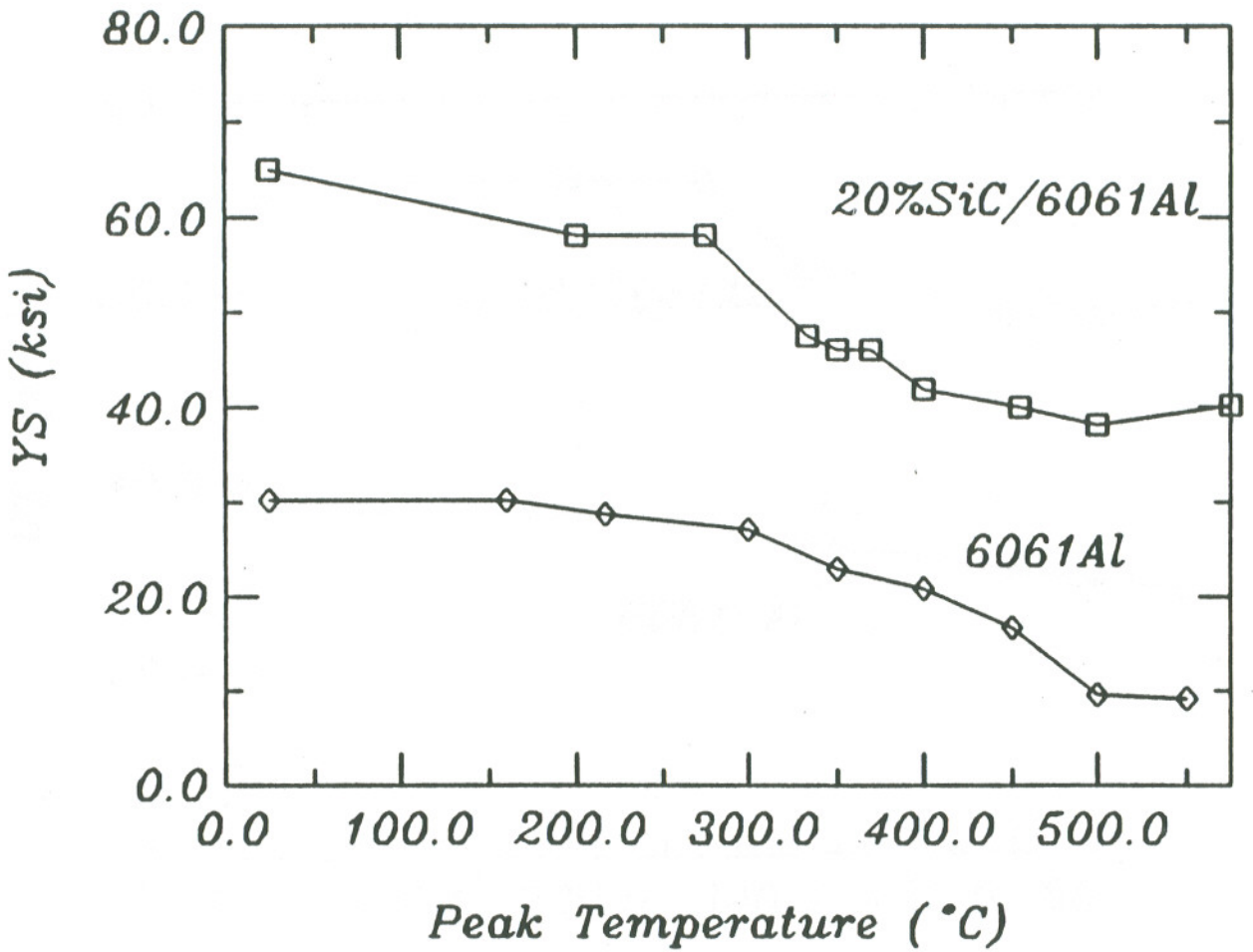

FIGURE 9 Variation in YS as a function of peak temperatures experienced in the HAZ

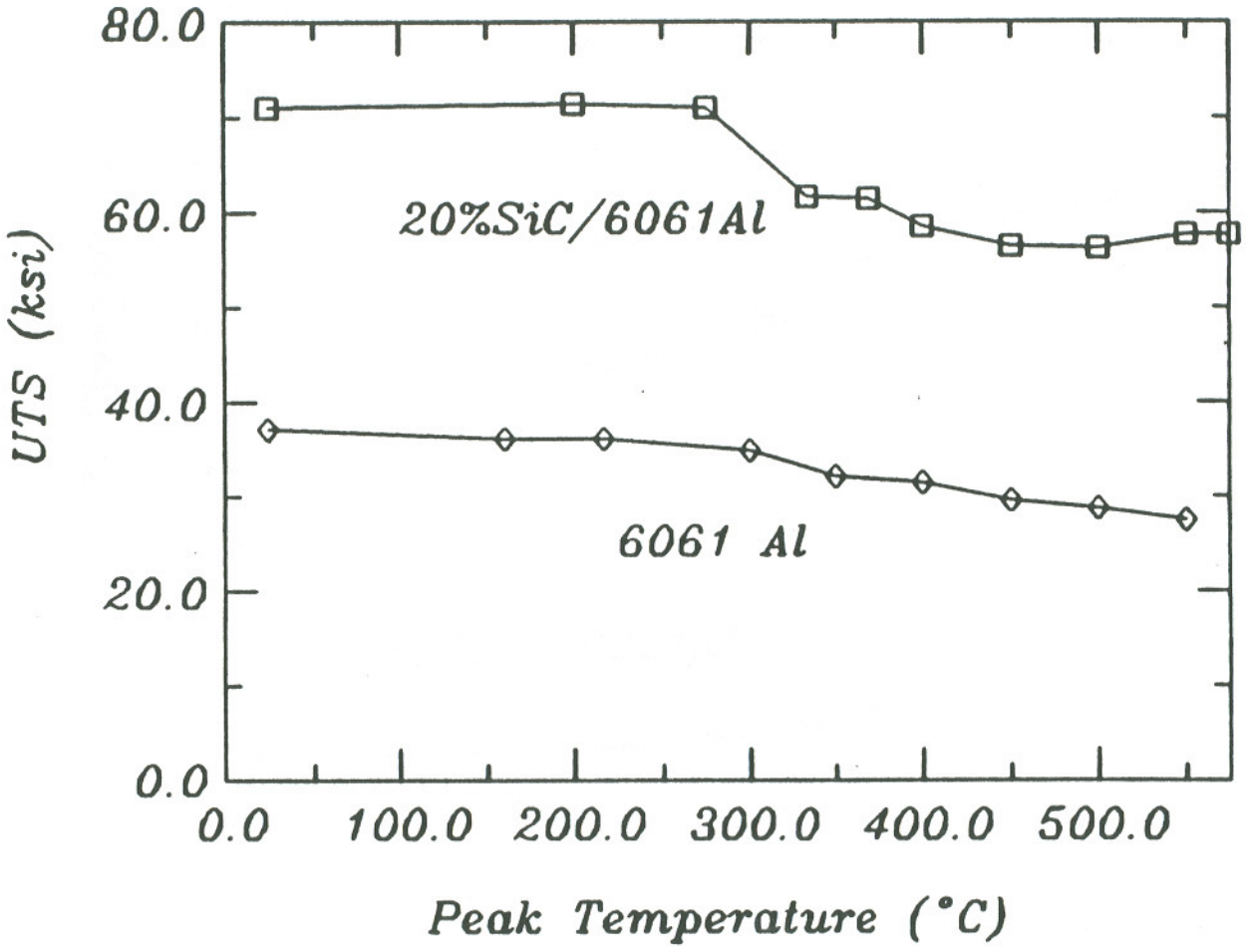

FIGURE 10 **Variation in UTS in the HAZ as a function of peak temperatures**

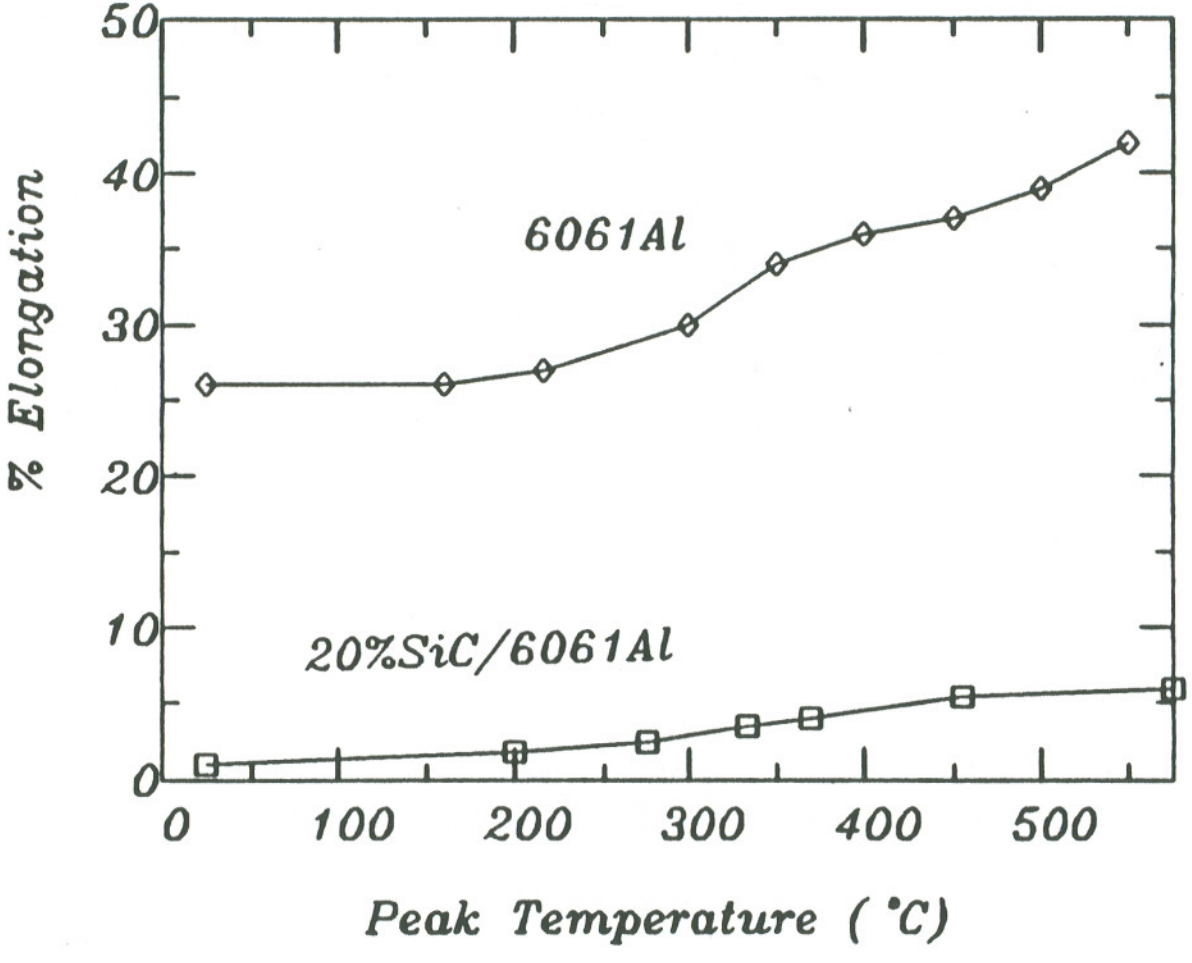

FIGURE 11 Variation in the percent elongation in the HAZ as a function of peak temperature.

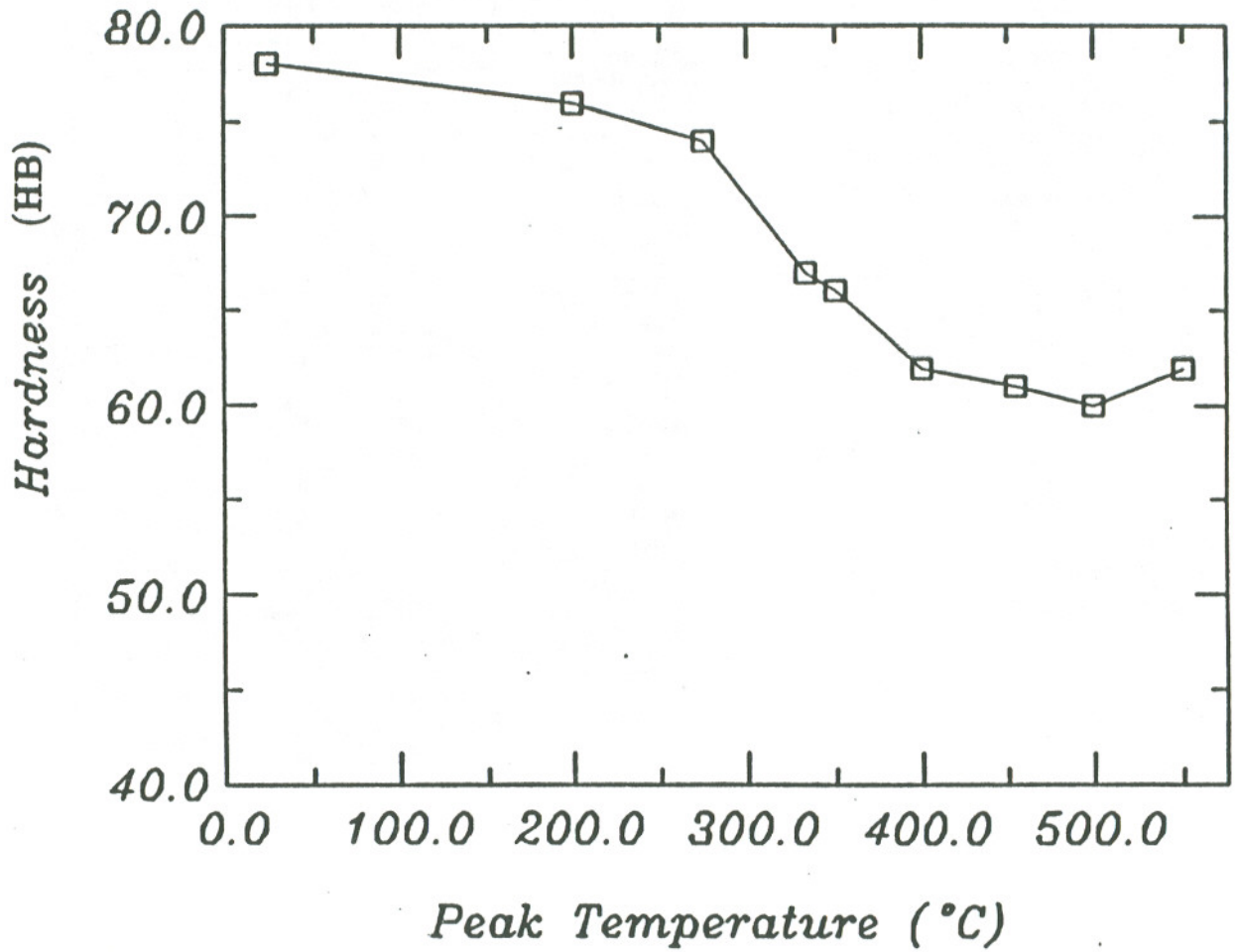

FIGURE 12 Variation in hardness of SiC/Al composite in the as a function of peak temperature

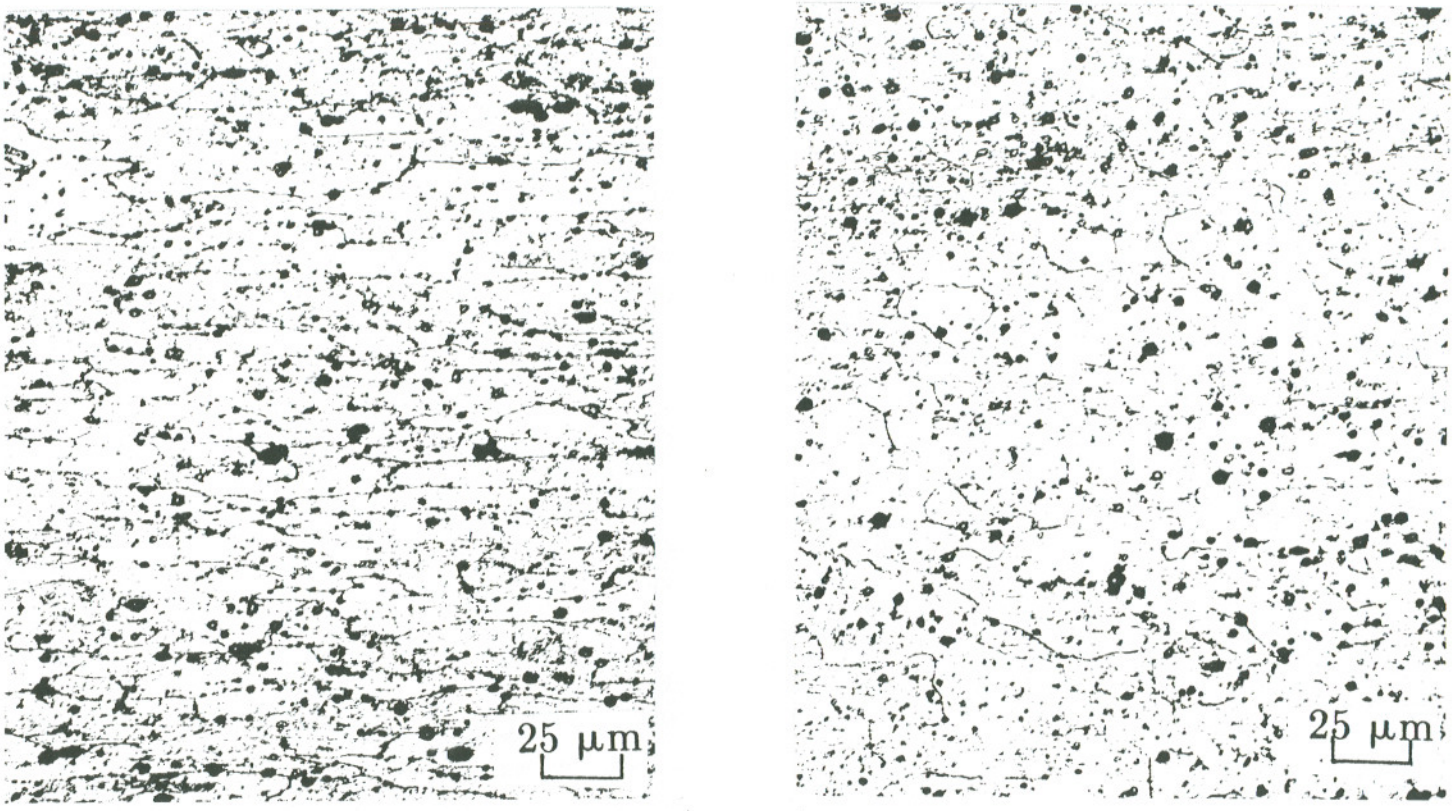

(a) (b)

FIGURE 13 a) Microstructure of 6061 Al in T6 condition
b) Microstructure in the HAZ experiencing a peak temperature of 500°C

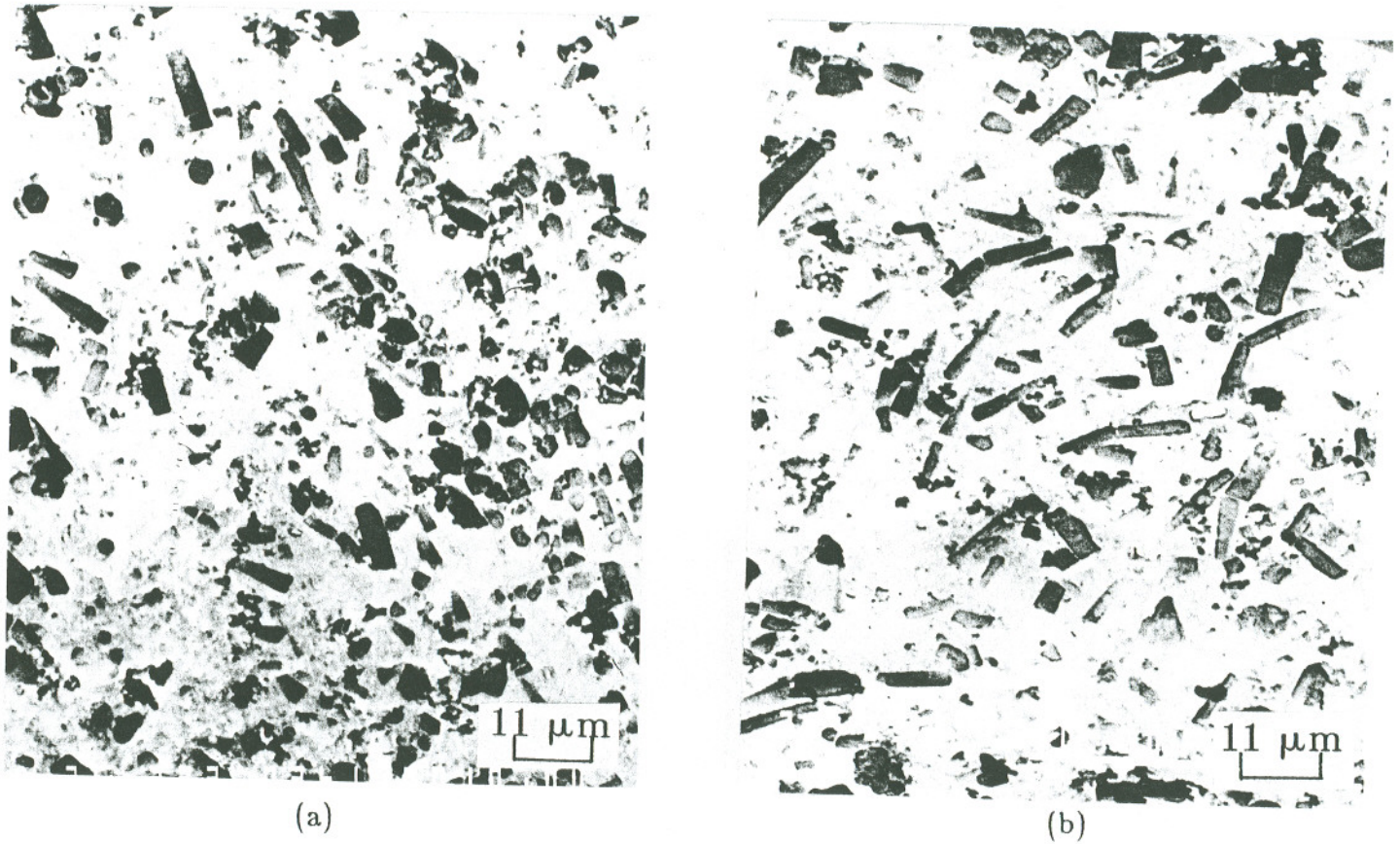

(a) (b)

FIGURE 14 Microstructures of SiC/Al in the as received condition
(a) Transverse section, (b) Longitudinal section

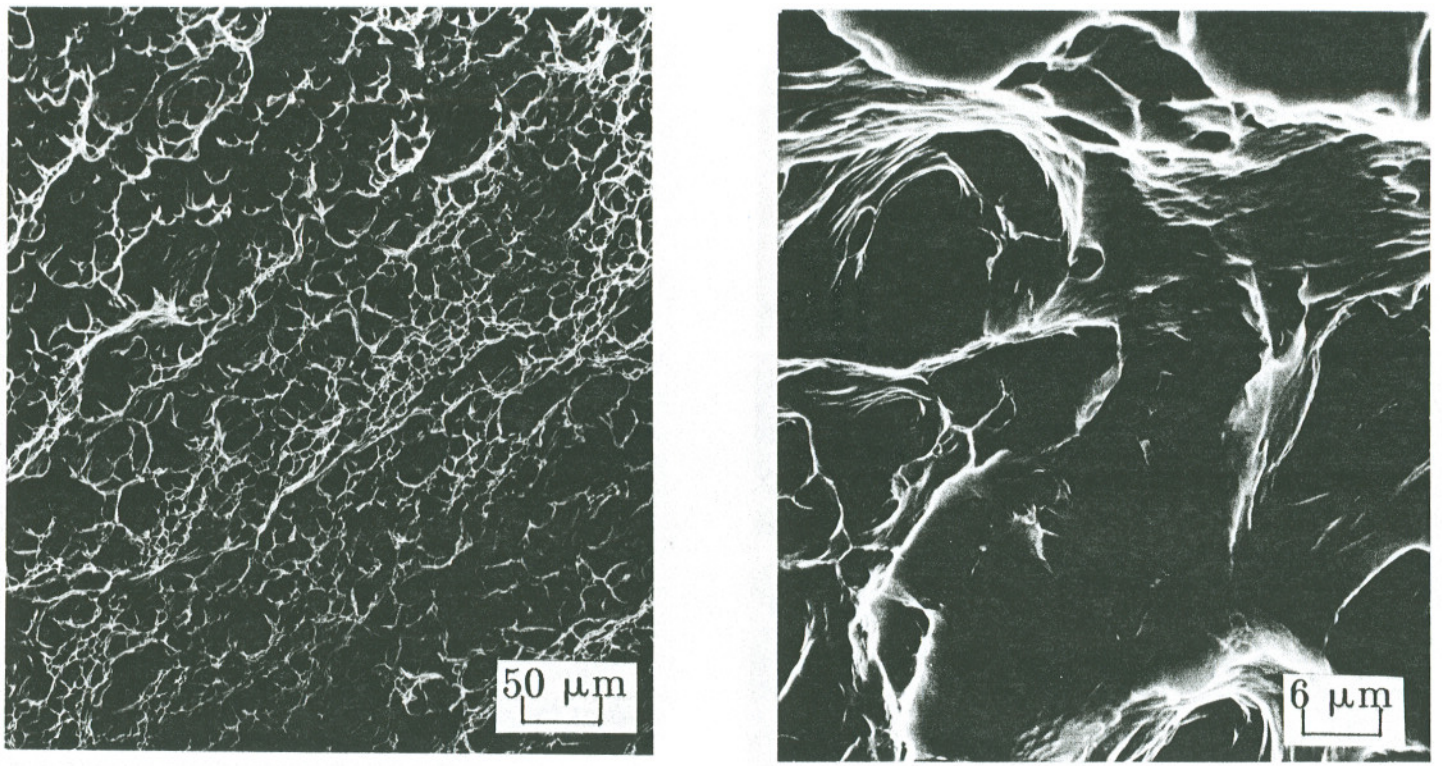

FIGURE 15 Fractographs of 6061 aluminum in T6 condition.

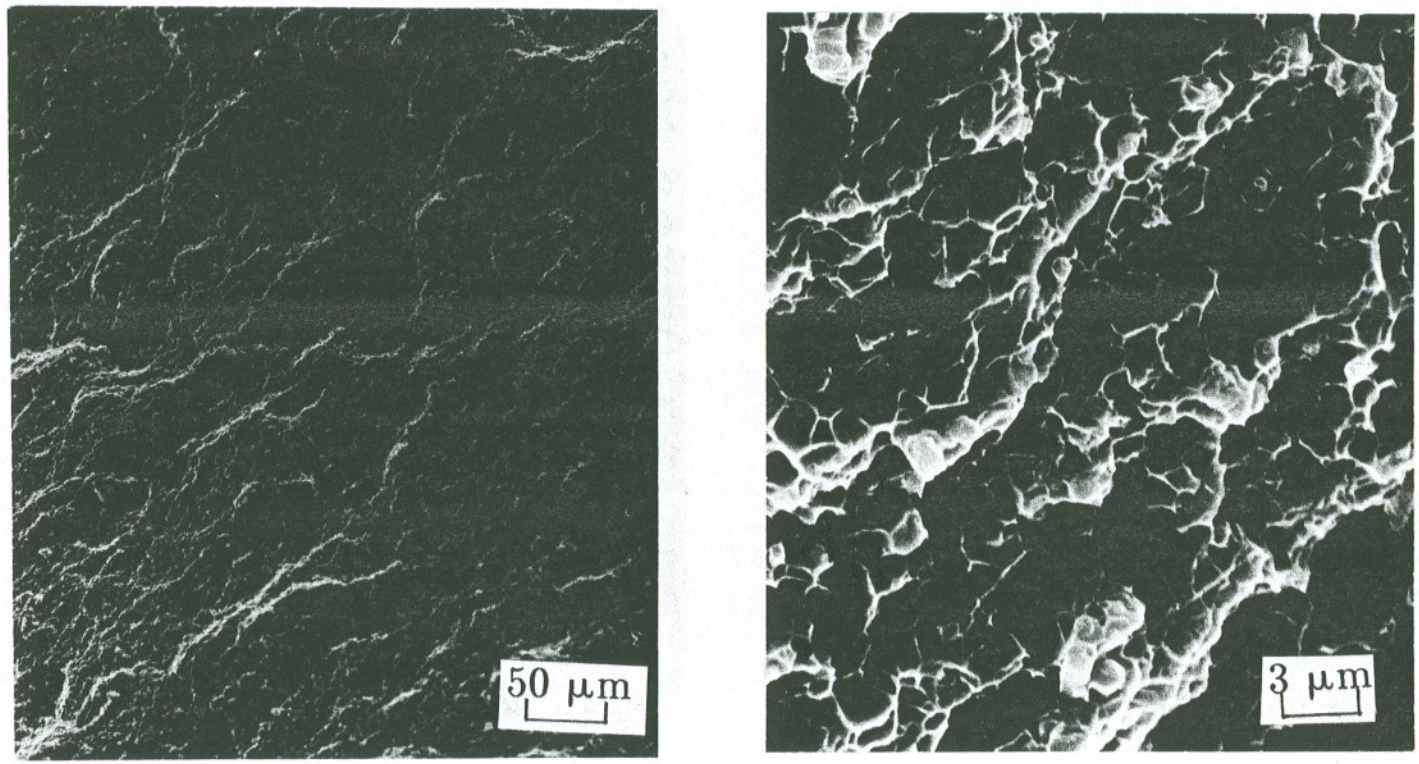

FIGURE 16 Fractographs of 20% SiC/6061 Al (T6) composite in as received condition

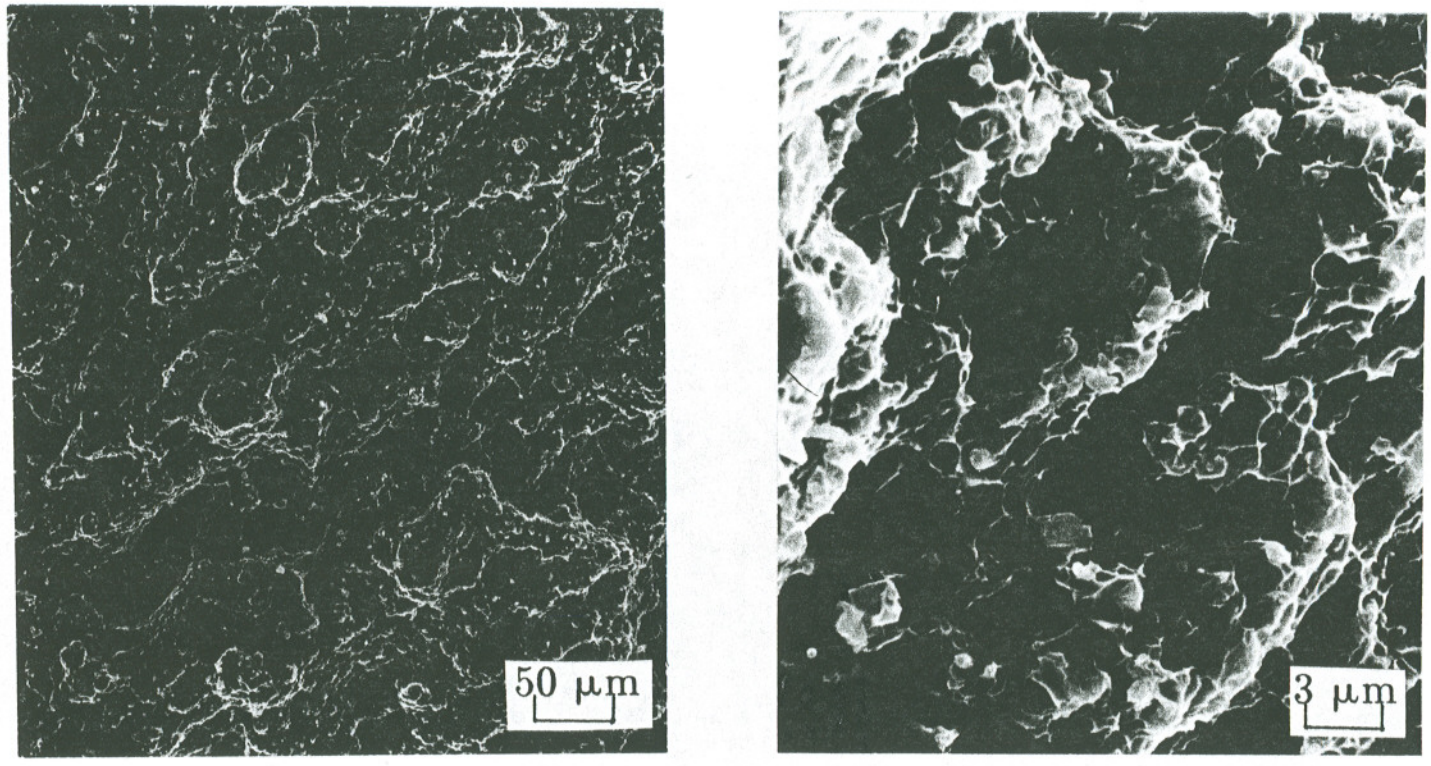

FIGURE 17 Fractograph of the SiC/Al in the HAZ after experiencing a peak tempereture of 500^{0}C

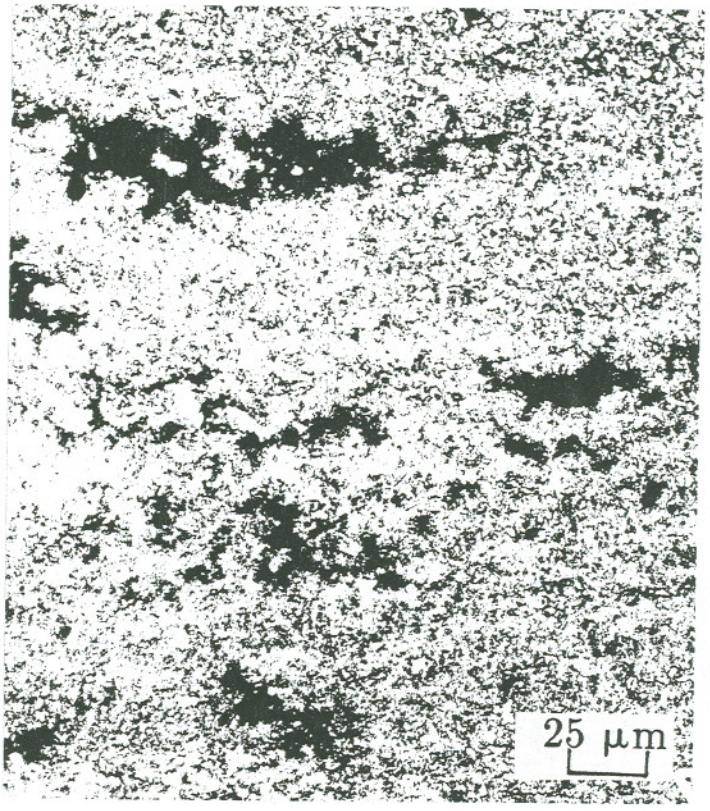

FIGURE 18 Microstructure of the composite showing porosity after holding it at 950°C for 15 minutes

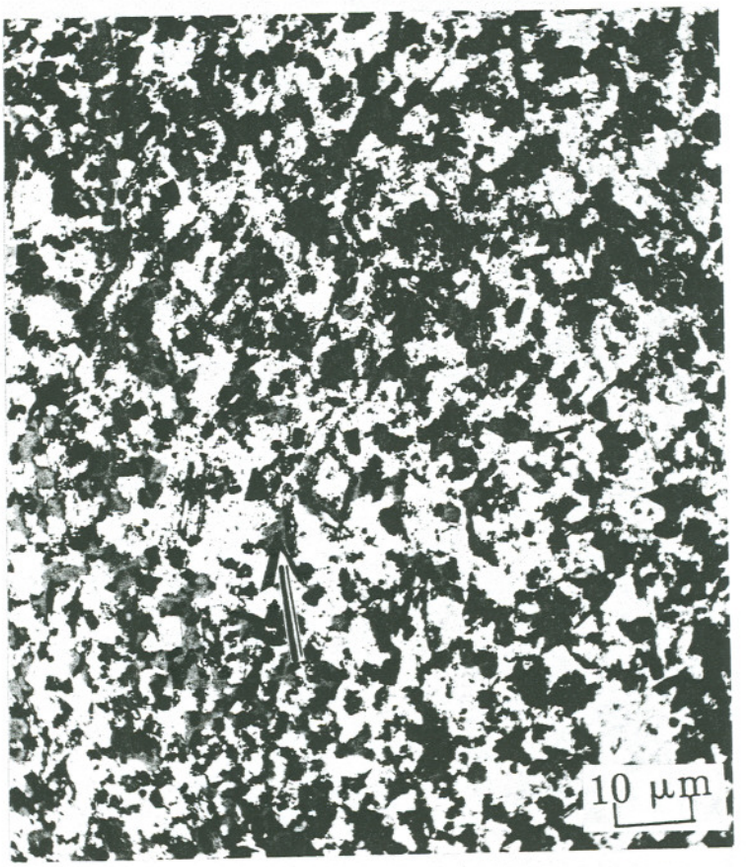

FIGURE 19 Microstructure of the composite (1100^0C,15min.) confirming the reaction between SiC (black) and Al matrix (white) leading to Si (grey) formation (indicated by arrow)

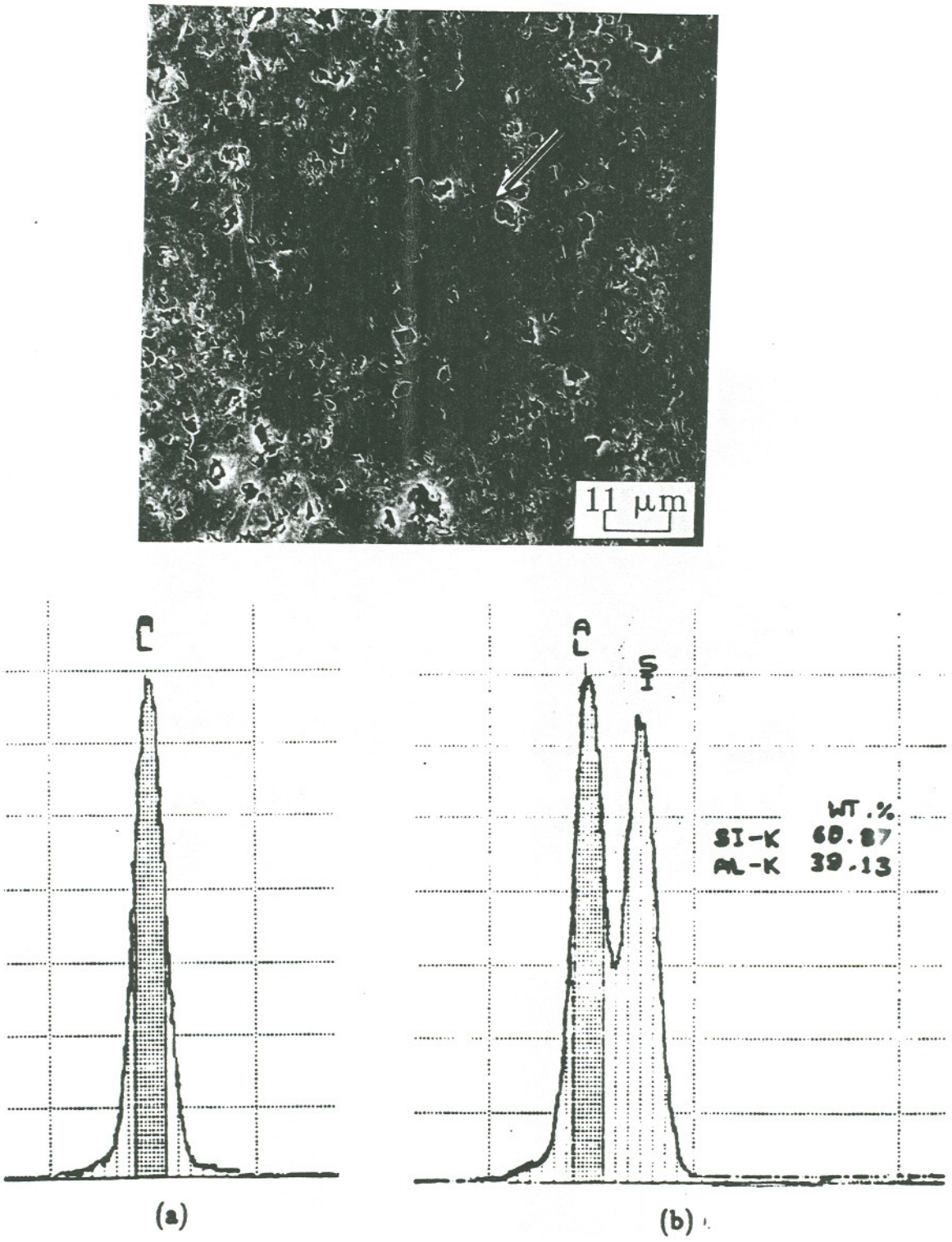

FIGURE 20 Energy dispersive X-ray analysis, (a) in the matrix and (b) in the dark region,(arrow) indicate that the reaction product is Si

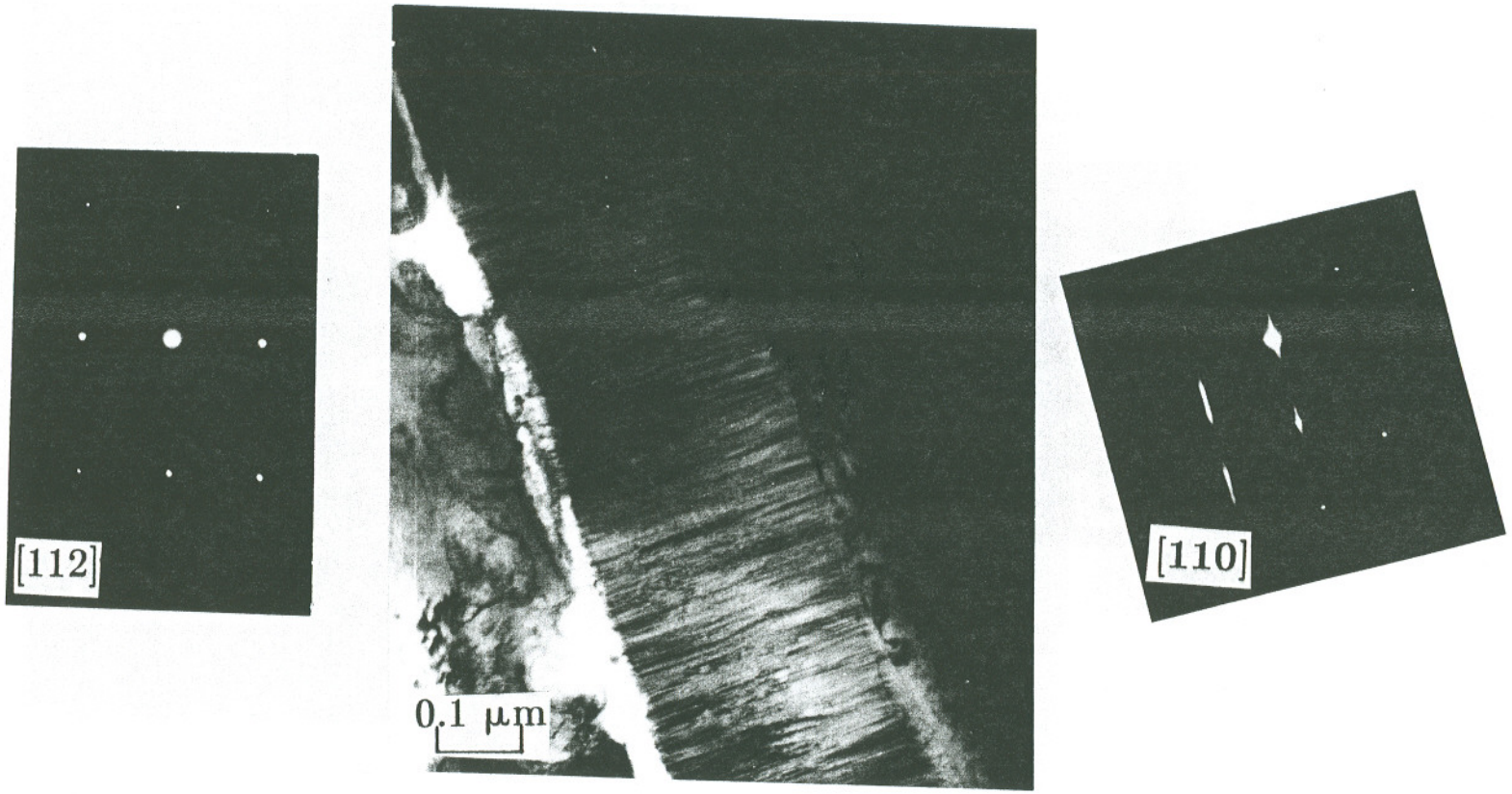

FIGURE 21. TEM micrograph of the composite with SAD pattern from SiC whisker at two different orientations.

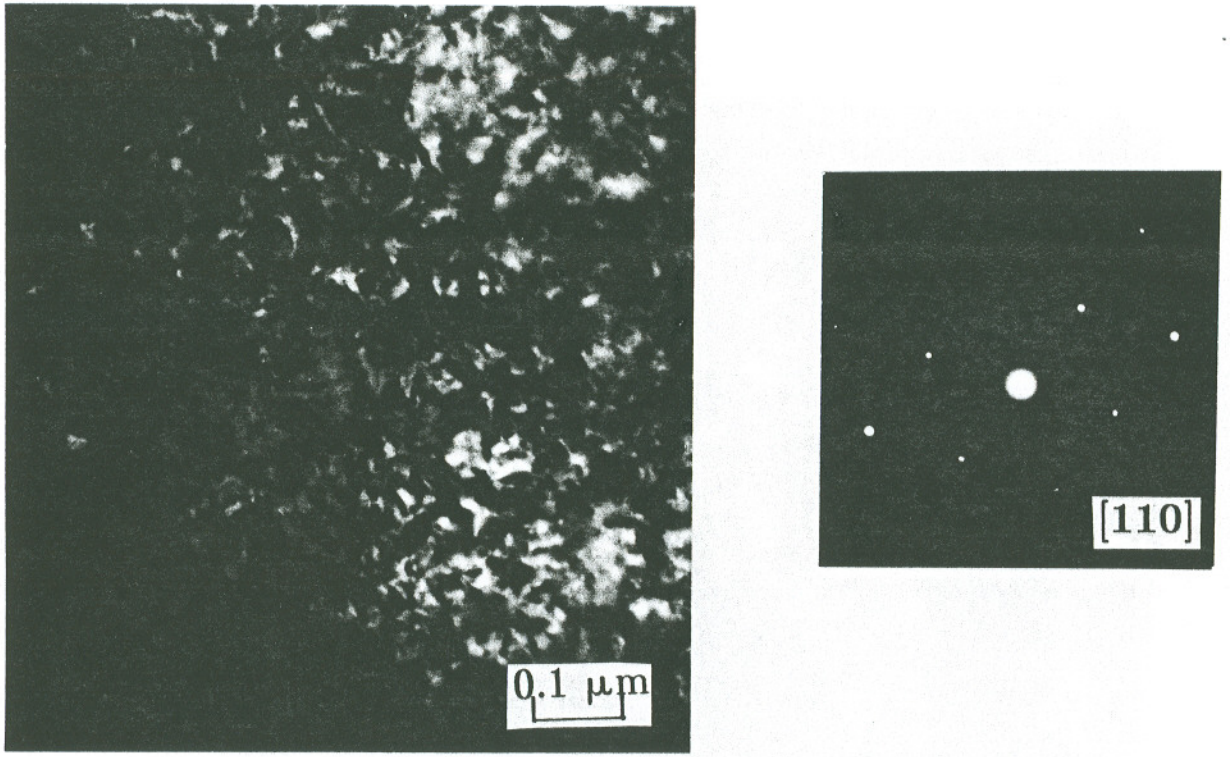

(a) (b)

FIGURE 22. **(a) TEM micrograph of SiC/Al matrix in T6 condition showing the heavily dislocated matrix decorated with precipitates, (b) SAD pattern**

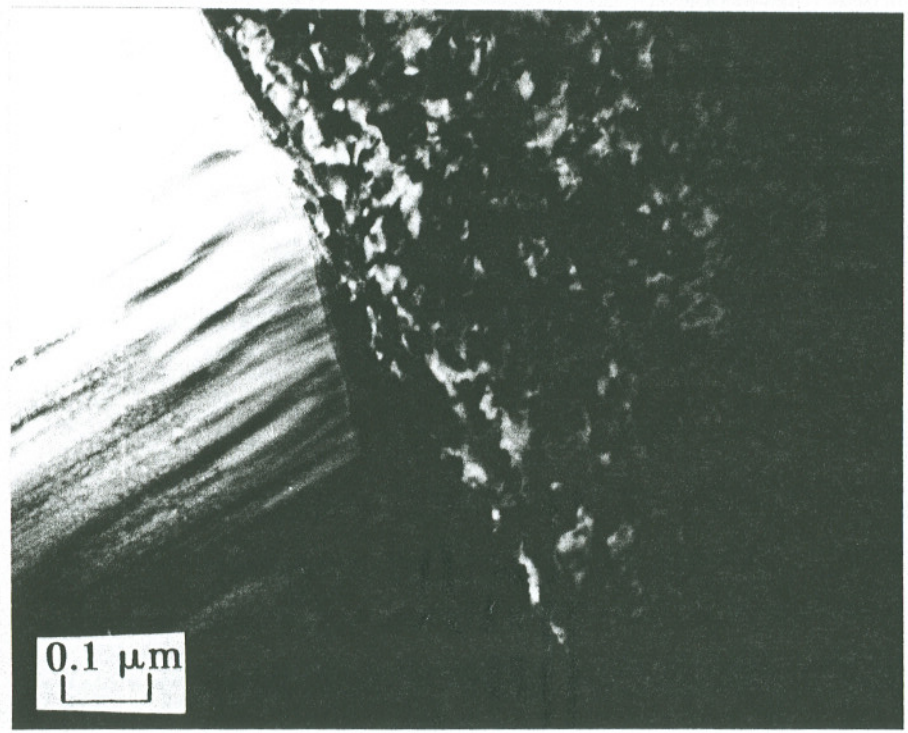

FIGURE 23. The SiC/Al interface in the composite in T6 condition

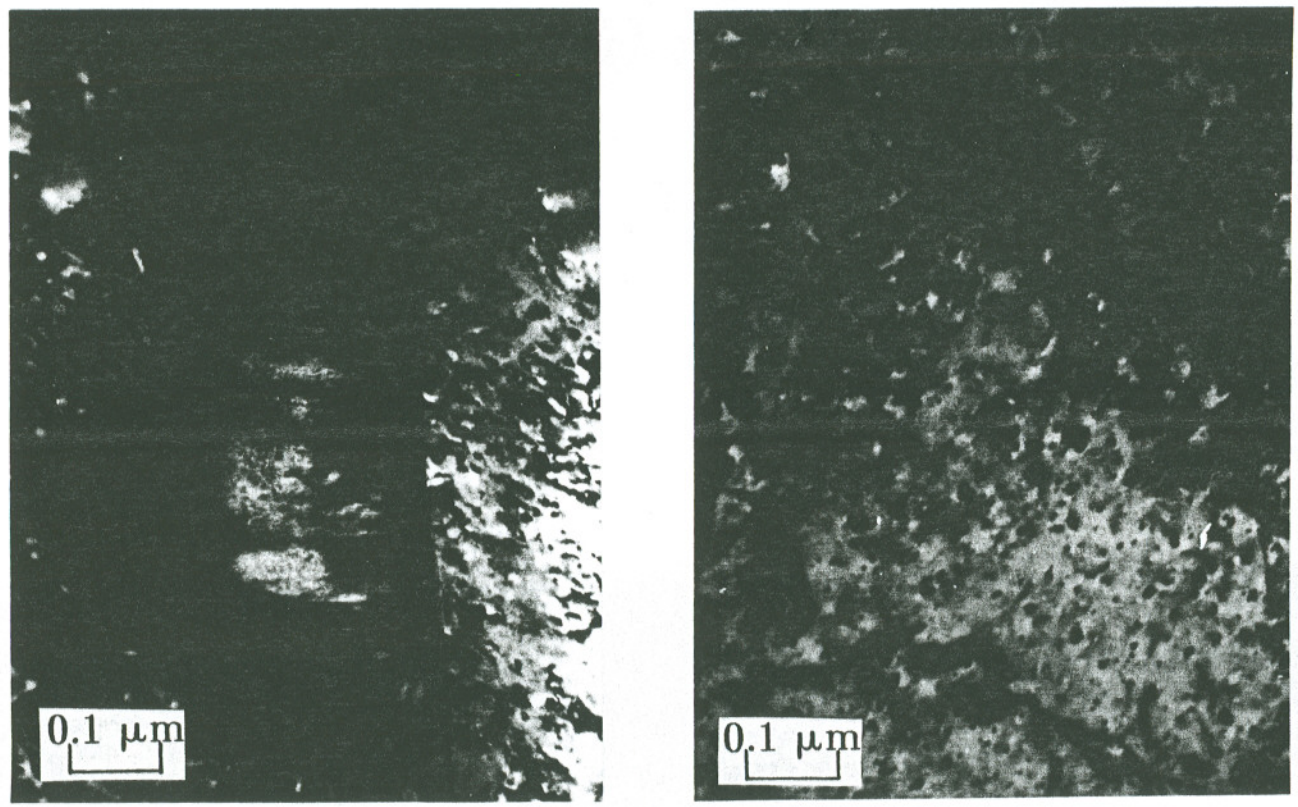

(a) (b)

FIGURE 24. **(a) TEM micrograph of the SiC/Al after exposure to 1100 °C, for 15min**
(b) the heavily dislocated matrix

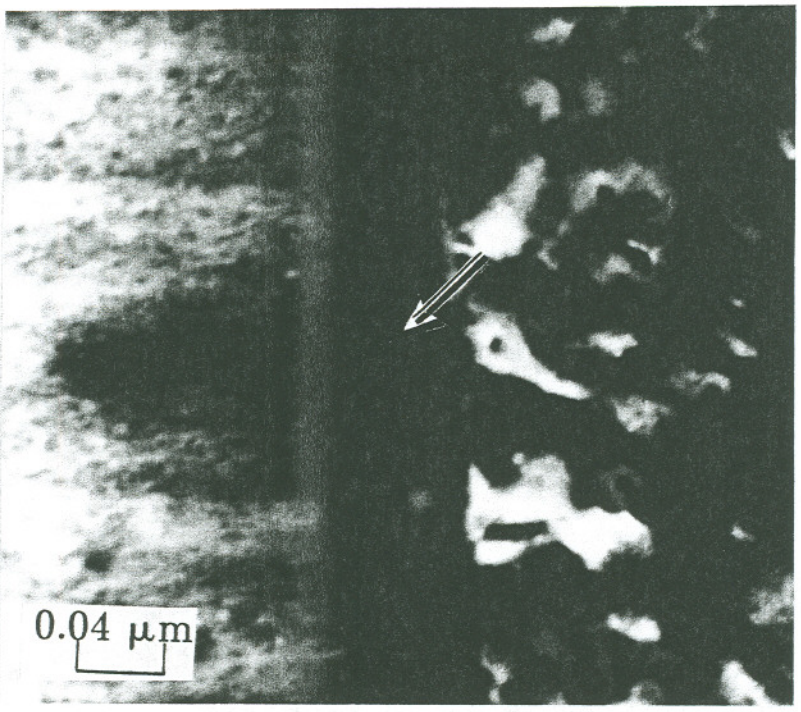

(a)

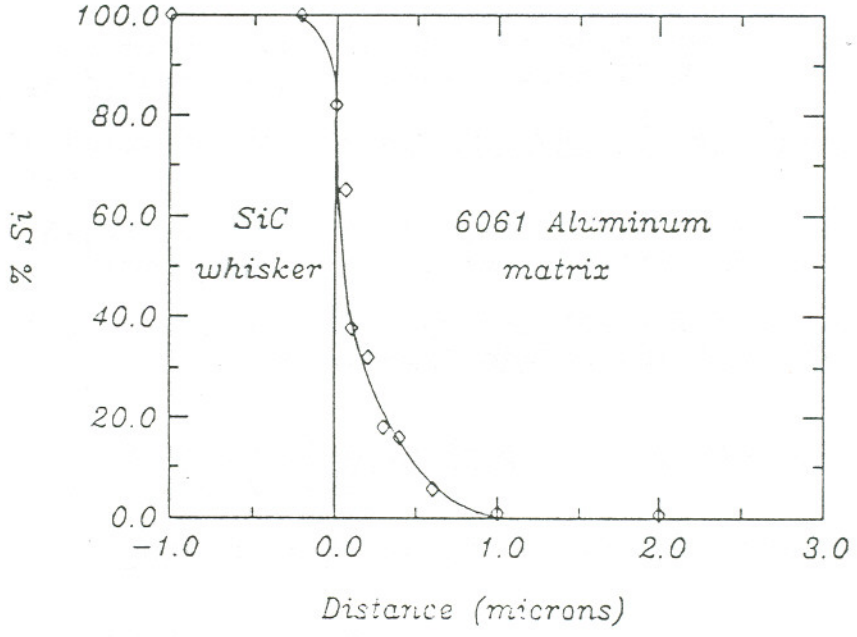

(b)

FIGURE 25. **(a) The interface after holding at 1100°C,15 min. (arrow pointing at the reaction product) (b) STEM EDAX Si profile from the whisker to within the matrix**

BIBLIOGRAPHY

1. Mody, P.B. and A.P. Majidi, "Metal matrix composites: The heat is on," Composite-In manufacturing, vol. 3, No. 1, 1987.

2. Divecha, A.P., S.G. Fishman, and S.D. Karmarkar, Journal of metals, pp. 12-17, Sept. 1987.

3. Dhingra, A.K., "Metal replacement by composites," Journal of metals, pp. 17-20, March 1980.

4. Harris, S.J., "Cast metal matrix composites," Materials science and technology, vol. 4, pp. 231-239, March 1988.

5. Ohuchi, K., H. Morimota, and T. Minamide, "Properties of SiC whisker reinforced Aluminum alloy composite," Kobelo Technology review, vol. No. 3, pp. 15-18, Feb. 1988.

6. McDanels, D.L., "Analysis of stress-strain fracture & ductility behaviour of aluminum matrix composites containing discontinous SiC reinforcement," Met. Trans. A, vol. 16A, pp. 1105-1115, June 1985.

7. Niskasen, P. and W.R. Mohn, "Versatile metal matrix composites," Metals Progress, pp. 39-41, March 1988.

8. Canon, P., "Aerospace materials," Journal of materials, pp. 10-16, May 1988.

9. Nieh, T.G., "Creep rapture in SiC reinforced aluminun composite," Metall. Tran. A, vol. 15A, pp. 139-146, Jan 1984.

10. Nair, S.V., J.K. Tien, and R.C. Bates, "SiC-reinforced aluminum metal matrix composites," Metals review, vol. 30, No.6, pp. 275-290, 1985.

11. Schoutens, J.E., Introduction to metal matrix composites, pp. 2-11, MMIAC, CA, June 1982.

12. Dieter, G.E., Mechanical Metallurgy, p. 233, McGraw-Hill, 1981.

13. Papazian, J.M., "Effects of SiC whiskers and particulate on precipitation in Al matrix composites," Met. Tran., vol. 19A, pp. 2945-2953, Dec. 1988.

14. Arsenault, R.J. and R.M. Fisher, "Microstructure of fiber and particulate SiC in 6061 Al composites," Scripta Meta., vol. 17, pp. 67-71, 1983.

15. Arsenault, R.J., "The strengthening of Al alloy 6061 by fiber and platlet SiC," Materials Science and Engineering, vol. 64, pp. 171-181, 1984.

16. Nutt, S.R. and R.W. Carpenter, "Non-equilibrium phase distribution in an Al-SiC composite," Materials Science and Engineering, vol. 64, pp. 171-181, 1984.

17. Christman, T. and S. Suresh, "Microstructural development in an Aluminum alloy-SiC whisker composite," Acta Meta., vol. 36, No. 7, pp. 1691-1704, 1988.

18. Vogelsang, M. and R.J. Arsenault, "An In-situ HVEM study of dislocation generation at SiC/Al interfaces in metal matrix composites," Metallurgical Transactions, vol. 17A, pp. 379-389, March 1986.

19. Li, S. and R.J. Arsenault, "Quantum Chemical study of adhesion at the SiC/Al interface," Journal of Applied Physics, vol. 68, No. 11, pp. 6246-6253, Dec. 1988.

20. Nutt, S.R., Interfaces in metal-matrix composites, edited by A.K. Dhingra & S.G. Fishman, pp. 157-167, The Metallurgical Society, Inc., PA, 1986.

21. Iseki, T., T. Kameda, and T. Maruyama, "Interfacial reaction between SiC and Al during joining," Journal of Materials Science, vol. 19, pp. 1692-1698, 1984.

22. Arsenault, R.J. and C.S. Pande, "Interfaces in metal matrix composites," Scripta Meta., vol. 18, pp. 1131-1134, 1984.

23. Cao, L., L. Geng, C.K. Yao, and T.C. Lei, "Interface in SiC whisker reinforced composites," Scripta Meta., vol. 23, pp. 227-230, 1989.

24. Nutt, S.R. and J.M. Duva, "A failure mechanism in Al-SiC composites," Scripta meta., vol. 20, pp. 1055-1058, 1986.

25. Jr., C.M. Adams, "Cooling rates and peak temperatures in fusion welding," Welding Journal, vol. 37 (5), pp. 210s-215s, 1958.

26. Weisman, Charlotte ed., "Heat flow in welding," Welding Handbook, Seventh edition, vol. 1, pp. 80-97, AWS, Miami, 1976.

27. Kou, S. and Y. Lae, "Three dimensional heat flow and solidification during autogenous GTA welding of Al plates," Metall. Tran., vol. 14A, pp. 2245-2253, Nov. 1983.

28. Kou, S., "Precipitation hardening materials,I: Alunimun alloys," Welding Metallurgy, pp. 277-289, John Wiley and Sons, Inc., 1987.

29. Kou, S., "Welding metallurgy and weldability of high strength Al alloys," Welding research council bulletin, vol. 320, WRC, N.Y., Dec. 1980.

30. Maitland, A.H. and A. Ried, "Metallurgical events in the heat-affected-zone of AlMgSi alloys," The first int. Al welding conference, pp. 106-114, WRC, Cleveland, OH, 1981.

31. Robertson, I. and J.B. Dwight, "HAZ softening in welded Al," Aluminum Weldments III, Proc. of third int. con. on Aluminum weldments, pp. II.1.1-.22, Aluminum-Verlog, Dusseldorf, 1985.

32. Kannikeshwaren, K. and R.Y. Liu, "Trace elements effect on Al-SiC interfaces," Journal of metals, pp. 17-19, Sept. 1987.

33. Nathan, M., "Interfacial reaction in metal matrix composites with a novel technique," Journal of Materials Science Letters, vol. 8, pp. 311-314, 1989.

34. Lloyd, D.J. and I. Jin, "A method of assesing the reactivity between SiC & molten Al," Metallurgical Transactions, vol. 19A, pp. 3107-3109, Dec. 1988.

35. Ahearn, J.S., C. Cooke, and S.G. Fishman, "Fusion welding of SiC-reinforced Al composites," Metal Construction, pp. 192-197, April 1982.

36. Devletian, J.H., "SiC/Al metal matrix composite welding using capacitor discharge process," Welding Journal, vol. 66, No. 6, pp. 33-39, Jan. 1987.

37. Moshier, W.C., J.S. Ahearn, and D.C. Cooke, "Interaction of Al-Si, Al-Ge and Zn-Al eutectic alloys with SiC/Al discontinously reinforced metal matrix composite," Journal of Materials Science, vol. 22, No. 1, pp. 115-122, 1987.

38. Devletian, J.H., Unpublished research, Oregon Graduate Center, 1984.

39. Katayama, S., R.D. Lundn, C. Swindeman, J.C. Danko, and T.McCay, "Modification of microstructure and properties in Al-SiC materials by Laser fusion welding technique," 2nd ASM int. con. on trends in welding research, Gatlenburg, TN, May, 1989.

Bibliographical Note

The author was born on February 3, 1966, in India. He attended Antonio Desouza High School and Ruia College, before joining department of metallurgical engineering at Indian Institute of Technology, Bombay, in 1983. He finished his Bachelor of technology in 1987 and subsequently joined Mukand Iron and Steel, Bombay.

He joined Oregon Graduate Center in sept. 1987 for pursuing his masters in materials science. He completed all the requirements for MS by June 1989.